

LMX1B is Essential for the Maintenance of Differentiated Podocytes in Adult Kidneys

Tillmann Burghardt,* Jürgen Kastner,* Hani Suleiman,* Eric Rivera-Milla,[†] Natalya Stepanova,* Claudio Lottaz,[‡] Marion Kubitza,* Carsten A. Böger,[§] Sarah Schmidt,^{||} Mathias Gorski,[¶] Uwe de Vries,* Helga Schmidt,* Irmgard Hertting,* Jeffrey Kopp,** Anne Rasclé,* Markus Moser,^{||} Iris M. Heid,^{¶††} Richard Warth,^{‡‡} Rainer Spang,[‡] Joachim Wegener,^{§§} Claudia T. Mierke,^{|||} Christoph Englert,[†] and Ralph Witzgall*

Institutes for *Molecular and Cellular Anatomy, [†]Functional Genomics, ^{‡‡}Medical Cell Biology, and ^{§§}Analytical Chemistry, University of Regensburg, Regensburg, Germany; [†]Leibniz Institute for Age Research, Fritz Lipmann Institute, Jena, Germany; Departments of [§]Internal Medicine II and [¶]Epidemiology and Preventive Medicine, University Hospital Regensburg, University of Regensburg, Regensburg, Germany; ^{||}Max-Planck-Institute of Biochemistry, Department of Molecular Medicine, Martinsried, Germany; ^{**}Kidney Disease Section, National Institute of Diabetes and Digestive and Kidney Diseases, National Institutes of Health, Bethesda, Maryland; ^{††}Institute of Epidemiology, Helmholtz Zentrum München, Neuherberg, Germany; and ^{|||}Institute of Experimental Physics I, University of Leipzig, Leipzig, Germany

ABSTRACT

Mutations of the *LMX1B* gene cause nail–patella syndrome, a rare autosomal-dominant disorder affecting the development of the limbs, eyes, brain, and kidneys. The characterization of conventional *Lmx1b* knockout mice has shown that LMX1B regulates the development of podocyte foot processes and slit diaphragms, but studies using podocyte-specific *Lmx1b* knockout mice have yielded conflicting results regarding the importance of LMX1B for maintaining podocyte structures. In order to address this question, we generated inducible podocyte-specific *Lmx1b* knockout mice. One week of *Lmx1b* inactivation in adult mice resulted in proteinuria with only minimal foot process effacement. Notably, expression levels of slit diaphragm and basement membrane proteins remained stable at this time point, and basement membrane charge properties also did not change, suggesting that alternative mechanisms mediate the development of proteinuria in these mice. Cell biological and biophysical experiments with primary podocytes isolated after 1 week of *Lmx1b* inactivation indicated dysregulation of actin cytoskeleton organization, and time-resolved DNA microarray analysis identified the genes encoding actin cytoskeleton-associated proteins, including *Abra* and *Arl4c*, as putative LMX1B targets. Chromatin immunoprecipitation experiments in conditionally immortalized human podocytes and gel shift assays showed that LMX1B recognizes AT-rich binding sites (FLAT elements) in the promoter regions of *ABRA* and *ARL4C*, and knockdown experiments in zebrafish support a model in which LMX1B and *ABRA* act in a common pathway during pronephros development. Our report establishes the importance of LMX1B in fully differentiated podocytes and argues that LMX1B is essential for the maintenance of an appropriately structured actin cytoskeleton in podocytes.

J Am Soc Nephrol 24: 1830–1848, 2013. doi: 10.1681/ASN.2012080788

Received August 9, 2012. Accepted May 21, 2013.

T.B., J.K., and H.S. contributed equally to this work.

Published online ahead of print. Publication date available at www.jasn.org.

Present address: Hani Suleiman, Department of Pathology and Immunology, Washington University, St. Louis, Missouri.

Present address: Anne Rasclé, Institute of Immunology, University of Regensburg, Regensburg, Germany.

Correspondence: Ralph Witzgall, University of Regensburg, Institute for Molecular and Cellular Anatomy, Universitätsstr. 31, 93053 Regensburg, Germany. Email: ralph.witzgall@vkl.uni-regensburg.de

Copyright © 2013 by the American Society of Nephrology

The analysis of several hereditary diseases has provided unequivocal evidence that podocytes assume a central role in the formation of the glomerular filtration barrier in the kidney. Every day, the kidney produces 180 L of primary filtrate, which is free of high molecular weight proteins and blood cells. To release only small molecules from the blood into the urine, the glomeruli contain a filtration barrier composed of endothelial cells, the glomerular basement membrane, and the podocytes. Whereas the contribution of the glomerular endothelial cells to the filtration properties is poorly understood, it is generally acknowledged that the basement membrane and the podocytes are essential components of the glomerular filter. In the case of podocytes, the filtrate moves through the slit diaphragm, a proteinaceous structure extending between neighboring foot processes that contains proteins such as nephrin, podocin, FAT1, CD2AP, Nck, and TRPC6. Despite the accumulating knowledge on the slit diaphragm, comparatively little is known on the genetic pathway responsible for podocyte development and maintenance of the fully differentiated podocyte.¹

Our studies focus on nail–patella syndrome, an autosomal-dominant hereditary disorder that is characterized by dysplastic nails, absent or hypoplastic patellae, open-angle glaucoma, and chronic nephropathy.² In 1998, the first mutations in *LMX1B*, a gene encoding a LIM homeodomain transcription factor, were reported to be responsible for nail–patella syndrome.^{3–5} With few exceptions,⁶ the more than 100 mutations described so far affect the protein binding LIM domains and the DNA binding homeodomain.^{6,7} The clinical manifestation shows a high variability in severity and penetrance,² which may be caused by the nature of the mutation or the presence of modifier genes. Ultrastructural analyses of the kidneys revealed a markedly thickened glomerular basement membrane with fibrillar inclusions and electron-lucent areas, thus creating a moth-eaten appearance.^{8,9} For a better functional understanding of *LMX1B*, the creation of a knockout mouse model was very helpful.¹⁰ It showed the importance of *LMX1B* for the development of foot processes and slit diaphragms in podocytes, and it led to the hypothesis that *LMX1B* regulates the synthesis of podocin and the $\alpha 3$ and $\alpha 4$ chains of collagen IV,^{11–13} three proteins playing an important role in the formation of the renal filtration barrier. However, type IV collagen chains and podocin were still present in biopsies from patients.¹⁴ This finding and the facts that (1) *Lmx1b* null mice die within 24 hours after birth and (2) nail–patella syndrome is inherited in an autosomal-dominant fashion, whereas *Lmx1b* (+/–) mice do not develop a phenotype¹³ emphasize the need for a better model system. It has been speculated that human patients suffer from haploinsufficiency, but it has not been ruled out that some of the mutant proteins acquire a new function or exert a dominant-negative effect.

To determine whether the death of the conventional *Lmx1b* knockout mice on the day of birth was caused by renal failure and specifically, a podocyte defect, we generated constitutive podocyte-specific *Lmx1b* knockout mice. Microdissection of

individual nephron segments showed that *Lmx1b* was only expressed in the glomerulus and no other nephron segment.¹⁵ Indeed, we observed that the podocyte-specific inactivation of *Lmx1b* led to postnatal death around 14 days after birth,¹⁵ thus confirming the essential role of *LMX1B* in podocytes. Remarkably, the synthesis of podocin, the $\alpha 4$ chain of collagen IV, and several other podocyte proteins was maintained in the constitutive podocyte-specific *Lmx1b* knockout mice, which argues against them being direct target genes of *LMX1B*. In addition, shortly after birth, no major structural defects were detected in podocytes; rather, it seemed that podocytes elaborated foot processes and slit diaphragms and lost them subsequent to the inactivation of *Lmx1b*.¹⁵ This finding prompted us to develop and characterize inducible podocyte-specific *Lmx1b* knockout mice to analyze the role of *LMX1B* in maintaining the differentiation status of podocytes.

RESULTS

Inactivation of *Lmx1b* in Adult Mice Leads to Early Proteinuria But Delayed Ultrastructural Changes and Apoptosis

We generated mice containing two floxed *Lmx1b* alleles together with an *NPHS2*-dependent reverse tetracycline-dependent transactivator (rtTA) and a tetO-dependent Cre expression cassette (for short, triple transgenic mice). Because of the action of the human *NPHS2* promoter fragment, the rtTA protein is only produced in podocytes.¹⁶ These mice represent a unique tool to investigate whether *Lmx1b* is necessary for the development of podocytes and to maintain their differentiation status. Triple transgenic mice with two floxed *Lmx1b* alleles showed no phenotype and were healthy without the induction of recombination. To determine the consequences resulting from the loss of *Lmx1b* in differentiated podocytes, doxycycline was administered to 3-month-old triple transgenic mice for 1, 2, and 4 weeks. Analysis of recombination at the *Lmx1b* locus by PCR was detected from the earliest time point, thus confirming our strategy (Figure 1A). None of the mice died in the first month after induction, but they developed strong albuminuria already after 1 week, which strongly suggested that the glomerular filtration barrier was affected on recombination of the *Lmx1b* gene (Figure 1, B and C).

It is generally agreed that the glomerular filtration barrier consists of the podocyte layer, the glomerular basement membrane, and possibly, the fenestrated endothelium lining the glomerular capillaries, although it is still a matter of debate how much the individual components contribute. We, therefore, wanted to find out what ultrastructural changes might underlie the proteinuria. Somewhat surprisingly, despite heavy proteinuria already after the first week of induction, only very occasional foot process effacement was observed by electron microscopy (Figure 2, A and B). The disappearance of foot processes became more pronounced at 2 weeks of induction (Figure 2, C and D) and was dramatic another 2 weeks later,

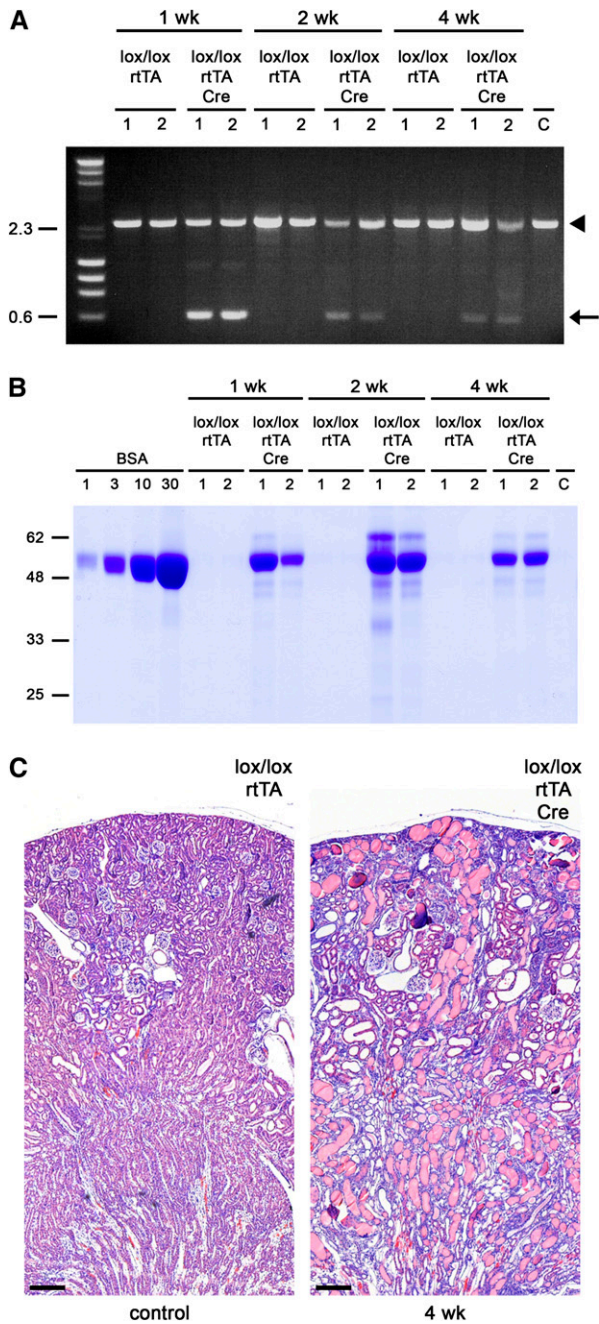


Figure 1. Podocyte-specific inactivation of *Lmx1b* leads to proteinuria. Mice of the indicated genotypes received doxycycline at a concentration of 2 mg/ml in the drinking water for 1, 2, and 4 weeks. (A) Total kidney genomic DNA was isolated from two animals each of the various mice. The *Lmx1b* allele after Cre-mediated recombination is indicated by an arrow, and the nonrecombined band is indicated by an arrowhead. C, triple transgenic mouse not receiving doxycycline. (B) Urine (0.2 μ l) from each of the indicated mice was analyzed on a 10% denaturing polyacrylamide gel together with 1, 3, 10, and 30 μ g BSA and then stained with Coomassie Brilliant Blue R250. Only triple transgenic mice treated with doxycycline developed proteinuria, and a triple transgenic mouse not receiving doxycycline served as a negative control (C). (C) A histologic section stained with

when podocytes had completely fallen off the capillaries (Figure 2E). Furthermore, erythrocytes had escaped into Bowman's space (Figure 2F). However, intact podocytes were found in all sections, even within glomeruli with severely misshaped podocytes, which is likely due to variable recombination in podocytes. Regrettably, our attempts to visualize *Lmx1b* by *in situ* hybridization and immunofluorescence with various mono- and polyclonal anti-*Lmx1b* antibodies failed. We were, therefore, not able to identify individual recombination events and correlate them with damaged podocytes. One possible reason for the loss of podocytes could be the induction of apoptosis. Indeed, by terminal deoxynucleotidyl transferase-mediated digoxigenin-deoxyuridine nick-end labeling (TUNEL) assay, we observed programmed cell death in podocytes and tubular cells, which was highest at weeks 1 and 2 (Figure 2H, and data not shown). The finding of apoptotic tubular cells probably is a secondary effect caused by the exposure of the tubular epithelium to the increased intraluminal concentration of proteins,¹⁷ because *Lmx1b* is not expressed in tubules.¹⁵ We wanted to confirm these *in vivo* findings by investigating the apoptosis rate in primary podocytes. However, no difference in the spontaneous apoptosis rate between podocytes from control and *Lmx1b* knockout animals was observed. We, therefore, exposed the cells to camptothecin, a drug known to induce apoptosis. This led to a markedly higher apoptosis rate in primary podocytes from the *Lmx1b* knockout mice (Supplemental Figure 1).

Onset of Proteinuria Cannot Be Explained by the Downregulation of Podocin and Collagen IV

In conventional *Lmx1b* knockout mice, the structural changes in podocytes and the glomerular basement membrane were proposed to be caused by the downregulation of collagen IV¹¹ and the slit diaphragm protein podocin.^{12,13} We, therefore, investigated whether podocin and collagen IV were also downregulated by the time proteinuria was observed in the triple transgenic mice. Remarkably, although pronounced proteinuria had developed after 1 week of doxycycline administration in the inducible *Lmx1b* knockout mice, it took another week for the downregulation of podocin, nephrin (another slit diaphragm protein), and the Wilms tumor protein 1 (Wt1) (a transcription factor mutated in several hereditary podocyte diseases) as determined by immunofluorescence (Figure 3A). It is, therefore, unlikely that proteinuria is caused by the loss of these proteins. In addition, the $\alpha 4$ chain of collagen IV was present during the whole time course (Figure 3A), which indicated that its synthesis was not affected as much or its turnover rate was lower than the turnover rate of the other proteins. The immunofluorescence data were confirmed by quantitative PCR, where we saw no statistically significant

hematoxylin/eosin shows the accumulation of proteins casts in the kidney of a triple transgenic mouse subjected for 4 weeks to doxycycline. Scale bars, 200 μ m.

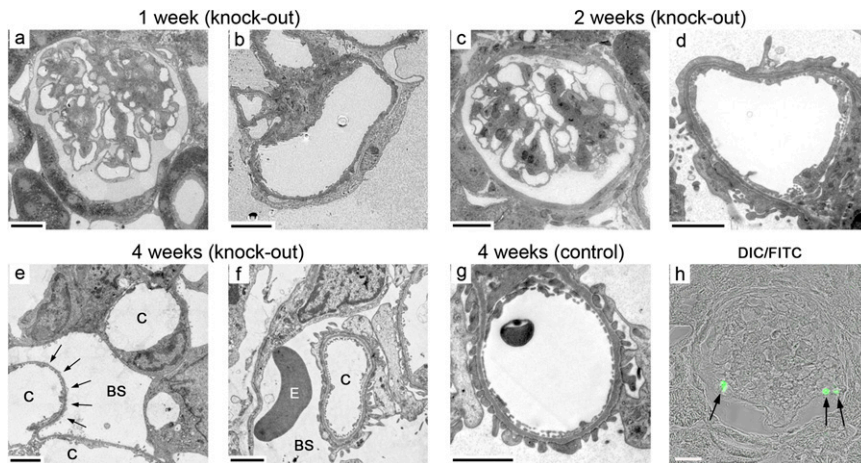


Figure 2. Ultrastructural changes and apoptosis after podocyte-specific inactivation of *Lmx1b*. Triple transgenic and control mice received doxycycline at a concentration of 2 mg/ml in the drinking water for the indicated times before they were perfusion-fixed and their kidneys were analyzed by transmission electron microscopy. (A and B) Glomerulus of a triple transgenic mouse exposed to doxycycline for 1 week. Foot process effacement was only detected in some capillary loops. (C and D) Triple transgenic mice exposed to doxycycline for 2 weeks lost foot processes over wide areas of the glomerular basement membrane. (E and F) Four weeks into the administration of doxycycline, (arrows in E) a completely denuded outer aspect of the basement membrane and (F) an erythrocyte outside of capillaries were seen. (G) A capillary loop of a Cre-negative control mouse receiving doxycycline for 4 weeks shows numerous foot processes. (H) TUNEL staining with FITC-labeled dUTP reveals apoptotic figures (arrows) in triple transgenic mice exposed to doxycycline for 1 week, and the differential interference contrast (DIC) picture shows their location at the periphery of the glomerular tuft. BS, Bowman's space; C, capillary; E, erythrocyte. Scale bars, 20 μ m in A, C, and H; 5 μ m in B; 2 μ m in D–G.

difference for *Nphs1*, *Nphs2*, *Cd2ap*, and *Wt1* mRNA levels (Figure 3B).

Because we could not rule out that additional basement membrane components, which we were not able to examine by immunofluorescence, could be affected by the inactivation of *Lmx1b*, we also investigated the charge composition of the glomerular basement membrane. It has been argued that not only the pore size but also the anionic charge of the basement membrane are responsible for its filter properties.¹⁸ Polyethyleneimine is a multicationic polymer that has been used to label anionic sites in the glomerular basement membrane.¹⁹ We induced the inactivation of *Lmx1b* and labeled the glomerular basement membrane with polyethyleneimine as soon as we noticed proteinuria (7 days of doxycycline administration). The anionic charge density was not different at this time between the proteinuric and nonproteinuric mice (Figure 3C), and therefore, the loss of anionic sites is unlikely to be responsible for the proteinuria.

Evidence for the Regulation of the Actin Cytoskeleton by *Lmx1b*

Because we were not able to identify any changes in slit diaphragm proteins or the glomerular basement membrane by

the time that proteinuria had developed after the inactivation of *Lmx1b*, we next turned our attention to cell-matrix contacts and the actin cytoskeleton. The inactivation of the genes encoding α 3- and β 1-integrin leads to podocyte foot process effacement,^{20–22} and integrins, just as slit diaphragm proteins, are connected to the actin cytoskeleton. Furthermore, mutations in the actin bundling protein α -actinin-4²³ and the inverted formin 2 (INF2)^{24,25} lead to hereditary FSGS, and inactivation of the actin-associated proteins synaptopodin²⁶ and cofilin-1²⁷ makes mice more susceptible to podocyte injury. Because of the fact that conditionally immortalized murine and human podocyte cell lines produce much reduced levels of *Lmx1b*/LMX1B compared with freshly isolated glomeruli, which was shown by Western blot analysis and real-time RT-PCR (data not shown), these cell lines were not suitable for additional analysis.

Preliminary experiments using stably transfected HeLa cells inducibly producing LMX1B, indeed, provided evidence that LMX1B influenced the migratory and adhesive behavior of these cells (data not shown). This result encouraged us to establish primary podocyte cultures of triple transgenic and control mice to look for defects in cell migration. These experi-

ments had to be performed soon after the isolation of the glomeruli, because the podocytes switched off the expression of *Lmx1b* in the course of cultivation (data not shown). Glomeruli were freshly isolated on the onset of proteinuria (7 or 8 days of induction) in the triple transgenic mice and seeded onto fibronectin-coated coverslips. When the outgrowth of podocytes was monitored 3 and 4 days after seeding of the glomeruli, it became clear that fewer glomeruli of the control mice had attached to the coverslip in the first place (data not shown). Furthermore, fewer podocytes per glomerulus grew out in the case of the control mice (Figure 4A). Quantitative real-time PCR confirmed that the cells growing out of the glomeruli in which Cre recombinase was induced synthesized less *Lmx1b* (Figure 4B). Additional experiments were carried out to determine whether primary podocytes adhere more strongly to the substratum in the presence of *Lmx1b*. Thirty minutes after replating, primary podocytes adhered more efficiently to laminin in the absence of *Lmx1b* (Figure 4C). These results prompted us to use a spectrum of cell biologic and biophysical techniques to obtain better insight how cell matrix contacts and the cytoskeleton are affected by the inactivation of *Lmx1b*.

Because potassium channels have been shown to play an important part in cell migration,²⁸ we first investigated

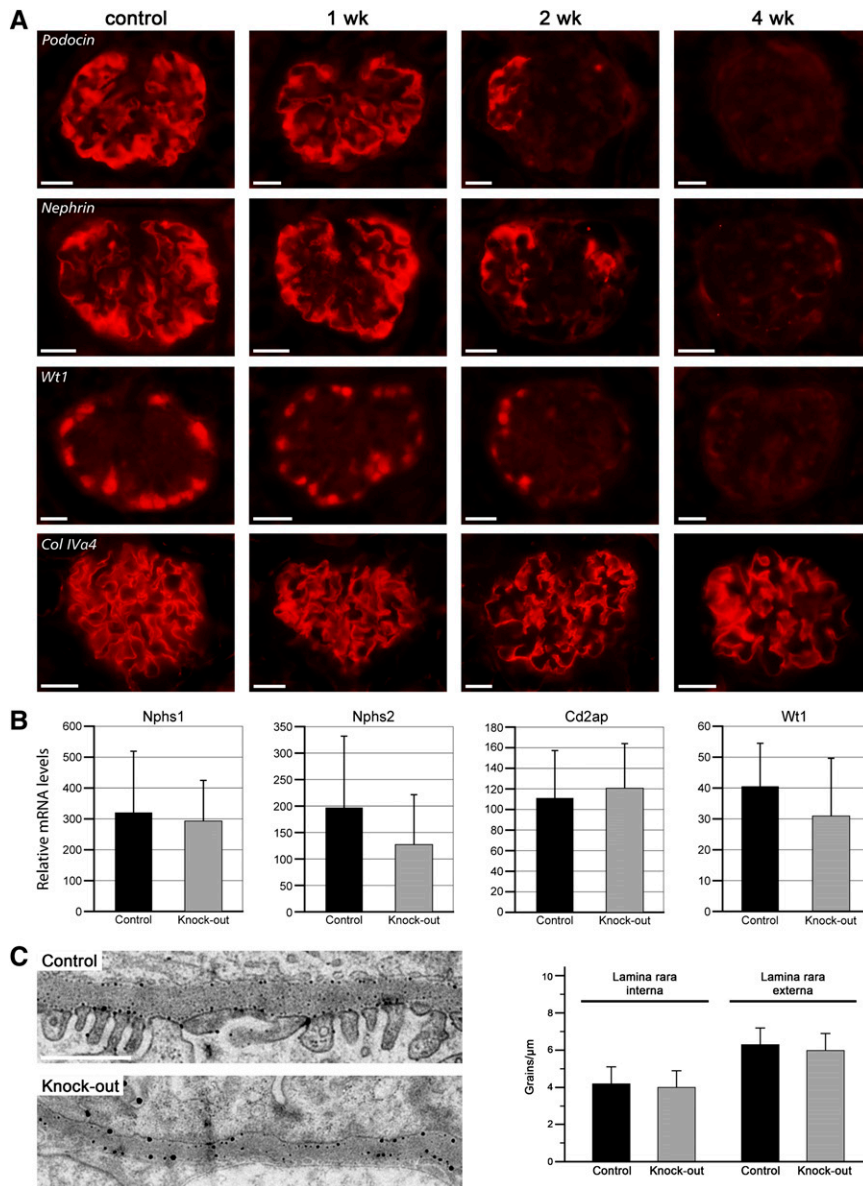


Figure 3. Expression of disease-associated genes and distribution of negative charges in the glomerular basement membrane after podocyte-specific inactivation of *Lmx1b*. (A) Triple transgenic mice received doxycycline at a concentration of 2 mg/ml in the drinking water for the indicated times before they were perfusion-fixed and their kidneys were immunofluorescence stained with the various antibodies. Whereas podocin, nephrin, and *Wt1* only disappear in triple transgenic mice exposed for 2 weeks to doxycycline, the $\alpha 4$ chain of collagen is still present even after 4 weeks. (B) Total RNA was isolated from the kidneys of animals receiving doxycycline for 7 days, and the respective mRNAs were quantitated by real-time PCR. No statistically significant difference was observed. (C) Mice were administered doxycycline for 7 days before the kidneys were removed without fixation, incubated with polyethyleneimine, and subjected to transmission electron microscopy. The polyethyleneimine-decorated glomerular basement membrane shows electron-dense deposits at the inner and outer aspects (the capillary lumen is located at the top and Bowman’s space is located at the bottom in C). As seen in the bar graph, the number of electron-dense grains per micrometer glomerular basement membrane was not different between control and knockout mice. Mice of the genotype *Lmx1b*^{lox/lox}; *Nphs2*:rtTA were used as controls. Shown are the mean values and SDs. Scale bars, 20 μ m in A; 1 μ m in C.

whether the effect of *Lmx1b* on cell motility was mediated through potassium channels. However, the membrane potential of primary podocytes was not statistically different between the control and the inducible knockout mice (Supplemental Figure 2). Similar results were obtained with podocytes still attached to freshly isolated glomeruli (data not shown). We then turned to the question of how fast podocytes spread on substrates after replating. Primary podocytes were seeded onto electrodes coated with BSA and fibronectin. The change of electrode capacitance during spreading is correlated with the spreading rate in a linear fashion, and the spreading rate, in turn, is directly proportional to the adhesion energy and inversely proportional to the cortical tension of the plasma membrane.²⁹ Not surprisingly, the spreading rate was much higher on fibronectin than BSA, but we did not observe a difference between podocytes with or without an inactivated *Lmx1b* gene (Figure 5A). This observation was consistent with the fact that the relative focal contact area as visualized by staining with an anti-paxillin antibody was the same in both podocyte populations (Figure 5B). Because we obtained no evidence that the function of focal contacts themselves is altered, we next asked whether the actin cytoskeleton is regulated by *Lmx1b*, which was done by analyzing the mobility of integrin complexes. Primary podocytes were incubated with fibronectin-coated nanobeads, and the movement of those beads was tracked by video microscopy. The beads attached to primary podocytes in which *Lmx1b* was deleted moved significantly less than the beads that were attached to primary podocytes with expression of *Lmx1b* (Figure 5C), thus arguing for a stiffer actin cytoskeleton. Such an assumption was supported by the stronger phalloidin staining of primary podocytes from *Lmx1b* knockout mice (Figure 5D). Furthermore, we were able to show a different recovery after destroying the actin cytoskeleton with cytochalasin. Primary podocytes from control animals recovered much faster after the removal of cytochalasin than the podocytes from *Lmx1b* knockout mice (Figure 5E).

These data show that *Lmx1b* regulates the organization of the actin cytoskeleton.

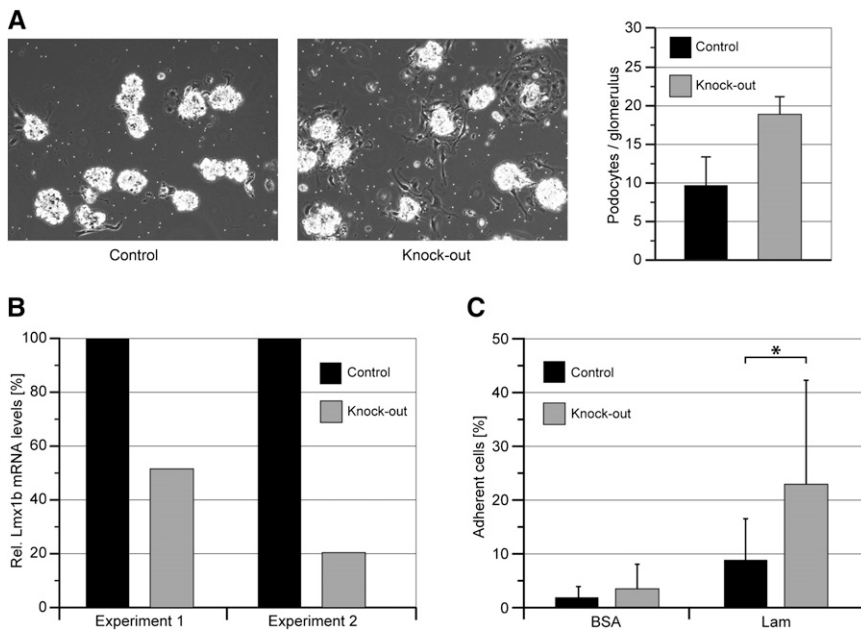


Figure 4. Outgrowth and adhesiveness of podocytes from control and knockout mice. Triple transgenic and *Lmx1b*^{lox/lox}; *NPHS2*:rtTA mice were administered 2 mg/ml doxycycline in the drinking water over a period of 7 days. (A) Glomeruli were isolated and cultured for 4 days to allow for the outgrowth of podocytes. More podocytes per glomerulus had grown out of glomeruli in which *Lmx1b* was inactivated. A total of 195 glomeruli and 1,842 podocytes was counted in the case of the control mice, and a total of 296 glomeruli and 5572 podocytes was counted in the case of the knockout mice. (B) To make sure that the podocytes growing out of the glomeruli of the triple transgenic mice indeed synthesized less *Lmx1b* mRNA, total RNA was isolated. Quantitative real-time PCR analysis shows reduced *Lmx1b* mRNA levels in podocytes cultured from Cre recombinase-positive mice. The data shown represent two independent experiments, in which two mice each (experiment 1) and six control mice and four knockout mice (experiment 2) were included. (C) Primary podocytes were trypsinized and replated into 96-well plates coated with BSA and laminin-111. Podocytes from knockout mice adhered better than those podocytes from control mice on laminin. Shown are the mean values and SDs. **P*<0.05.

To obtain molecular insight into the pathway(s) regulated by LMX1B, we performed a microarray analysis of glomeruli collected at various time points after the addition of doxycycline. Mice without Cre but receiving doxycycline served as a negative control. Potential candidate genes should fulfill the following criteria: (1) they should not be regulated by doxycycline (*i.e.*, their level should not change in the Cre-negative mice), (2) they should be increasingly regulated the longer the administration of doxycycline lasted, because mild proteinuria was observed after 5 days and pronounced proteinuria was observed after 7 days (Figure 6, A and B), and (3) they should be regulated at least twofold on day 7 that required a false discovery rate of 1% for the detection of differential expression. Altogether, only seven genes fulfilled our criteria: five genes were upregulated, and two genes were downregulated after the inactivation of *Lmx1b* (Figure 6, C–I). The five upregulated genes encode transgelin (*syn.* SM22 α), *Gadd45 β* , *Tnfrsf12a* (member 12a of the TNF receptor

superfamily, *syn.* Fn14, TWEAK receptor), the protease *Pamr1*, and *Crct1*, a protein of unknown function. The two downregulated genes encode dendrin and semaphorin-3g. Transgelin is associated with the actin cytoskeleton and stabilizes stress fibers,³⁰ *Tnfrsf12a* can be induced by RhoA and ROCK,³¹ dendrin has been localized to the slit diaphragm,^{32,33} and dendrin,³³ *Tnfrsf12a*³⁴ and *Gadd45 β* ³⁵ are proapoptotic proteins. Because these genes were promising candidate target genes for *Lmx1b*, we wanted to confirm the microarray data by quantitative real-time PCR. Glomeruli were isolated immediately before the administration of doxycycline and after 7 days of continuously administering doxycycline in the drinking water. *Lmx1b* mRNA levels had dropped to 40% in the Cre-positive glomeruli compared with the Cre-negative glomeruli (Figure 7A). At the same time point, the mRNA levels of transgelin had risen to 799%, those of *Gadd45 β* had risen to 211%, and those of *Tnfrsf12a* had risen to 318%, whereas dendrin mRNA levels had fallen to 33% of control levels (Figure 7A). The real-time PCR results, therefore, corroborated the microarray data and encouraged us to analyze additional genes that had not fulfilled our stringent criteria completely, because their levels varied less than twofold in the DNA microarray analysis. By quantitative real-time PCR, we were able to show that the mRNA levels of actin binding Rho-activating protein (*Abra*; *syn.* Stars) and *Arl4c* (*syn.* *Arl7*) had risen to 519% and 578% of control

levels, respectively (Figure 7A). To determine the functional significance of the putative target genes, we transiently transfected primary podocytes with expression plasmids for *Abra*, *Arl4c*, and *Crct1*. Subsequent staining with phalloidin revealed that the transfected cells showed stronger fluorescence, which indicated that those proteins led to the increased formation of F-actin (Figure 7B). Additional confirmation of the microarray data was sought by immunofluorescence staining of kidney sections. Because the transgelin mRNA was induced strongest among the mRNAs tested and suitable antibodies were available for the transgelin protein, we chose to investigate transgelin. In the presence of *Lmx1b*, glomeruli did not stain positive, whereas after the inactivation of *Lmx1b*, a strong signal for transgelin was seen. Double staining for the podocyte marker synaptopodin confirmed that transgelin was induced in podocytes (Figure 7C).

LMX1B has been shown to recognize adenine and thymine-rich binding sites in the promoter region of its target genes, the Far-linked AT-rich (FLAT) element.^{11–13,36,37} To show that the genetic changes observed in the inducible *Lmx1b* knockout mice were

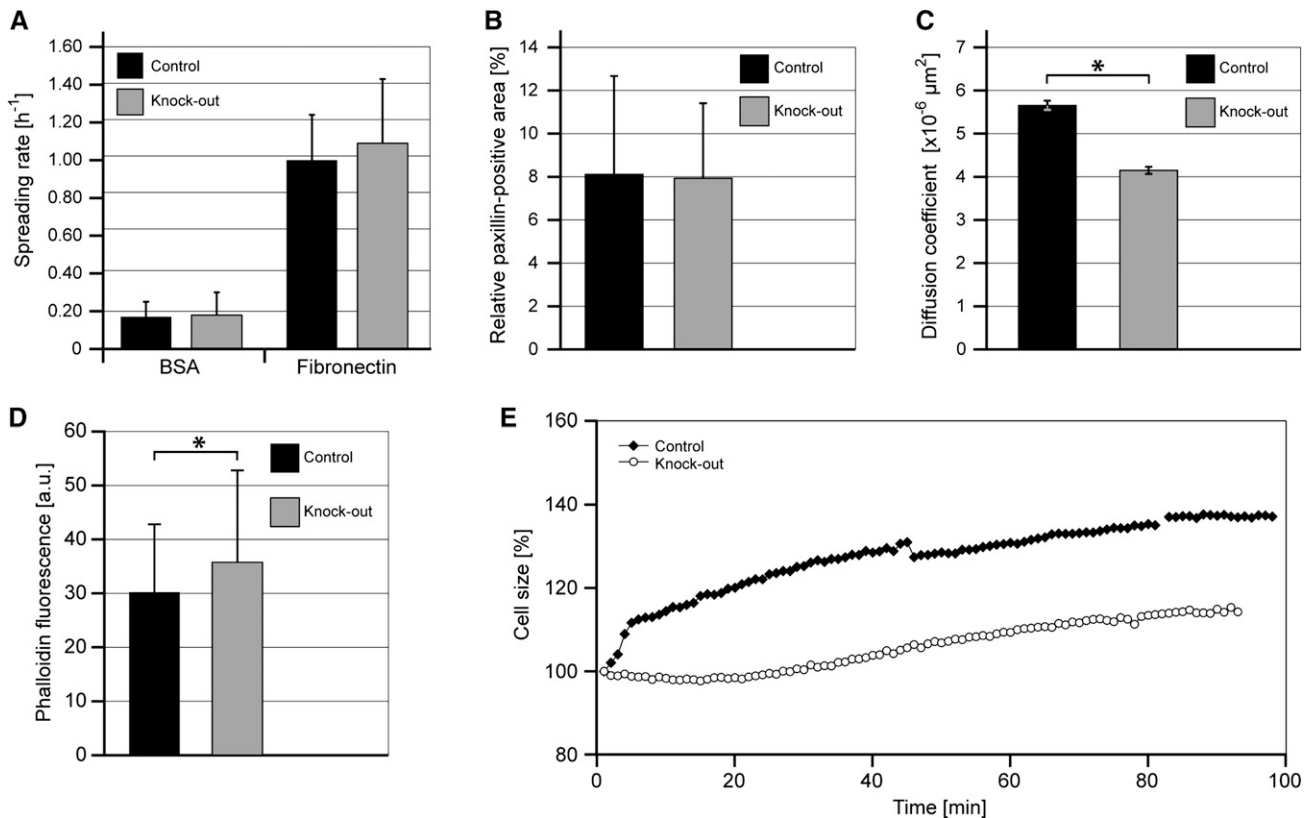


Figure 5. Characterization of primary podocytes. Glomeruli were isolated from triple transgenic and *Lmx1b*^{lox/lox}; *NPHS2:rtTA* mice that had received 2 mg/ml doxycycline in the drinking water over a period of 7 days. Primary podocytes were used 5–6 days after the isolation of glomeruli. (A) Primary podocytes were subjected to electric cell substrate impedance sensing. A statistically significant difference in the spreading rate observed was not observed on either BSA or fibronectin. (B) Immunofluorescence staining with an antipaxillin antibody was used to visualize cell matrix contacts. No difference can be seen between the focal contact area of podocytes isolated from the triple transgenic mice and the area of podocytes from control mice. The numbers shown reflect measurements from 27 to 31 cells each of three knockout and three control mice. (C) The random movement of fibronectin-coated nanobeads attached to the primary podocytes was tracked by video microscopy. Nanobeads moved significantly less on podocytes isolated from the knockout mice as judged by the diffusion coefficient; 1805 particles were tracked in the podocytes of control mice, and 1863 particles were tracked in the podocytes of knockout mice. (D) Primary podocytes were stained with fluorescently labeled phalloidin to visualize the F-actin cytoskeleton. Cells isolated from knockout mice showed stronger phalloidin staining (a.u., arbitrary units). (E) F-actin was destroyed by incubation with 5 μ g/ml cytochalasin for 24 hours. The average cell size at this time point was taken as 100%. Then, cytochalasin was removed, and pictures were taken every 60 seconds. Primary podocytes from control mice spread out much faster after the removal of cytochalasin than the podocytes from knockout mice. Shown are the mean values and SDs, except for C, which shows the geometric mean plus SEM. * $P < 0.05$.

caused by a direct binding of LMX1B to the promoter regions of the respective genes, chromatin immunoprecipitation (ChIP) assays were carried out. Because we wanted to analyze up to 6,000 bp upstream of the transcriptional start site for functional FLAT elements and freshly isolated glomeruli represented scarce material, we first made use of stably transfected HeLa cells inducibly producing human LMX1B to scan the promoter regions. Although we were not able to identify a FLAT element recognized by LMX1B in the promoter region of the *TAGLN* gene (the gene encoding transgelin), we found two closely spaced FLAT elements for the *ABRA* gene and one FLAT element for the *ARL4C* gene to which LMX1B was able to bind (Figure 8A). This finding encouraged us to carry out ChIP experiments with isolated mouse glomeruli to show binding of the

endogenous *Lmx1b* protein to the homologous FLAT elements of the murine *Abra* and *Arl4c* promoter regions. Regrettably, our ChIP assay was not sensitive enough to show binding of *Lmx1b* to these FLAT elements in podocytes of freshly isolated glomeruli. Therefore, we transiently transfected conditionally immortalized human podocytes with an expression plasmid for the human LMX1B protein and subjected them to ChIP. Indeed, we were now able to show binding of LMX1B to the respective FLAT elements in the promoter regions of both the *ABRA* and *ARL4C* genes (Figure 8B). The results of the ChIP experiments were confirmed by gel shift assays. Using recombinant human LMX1B protein, we showed specific binding of LMX1B to these FLAT elements (Figure 8C).

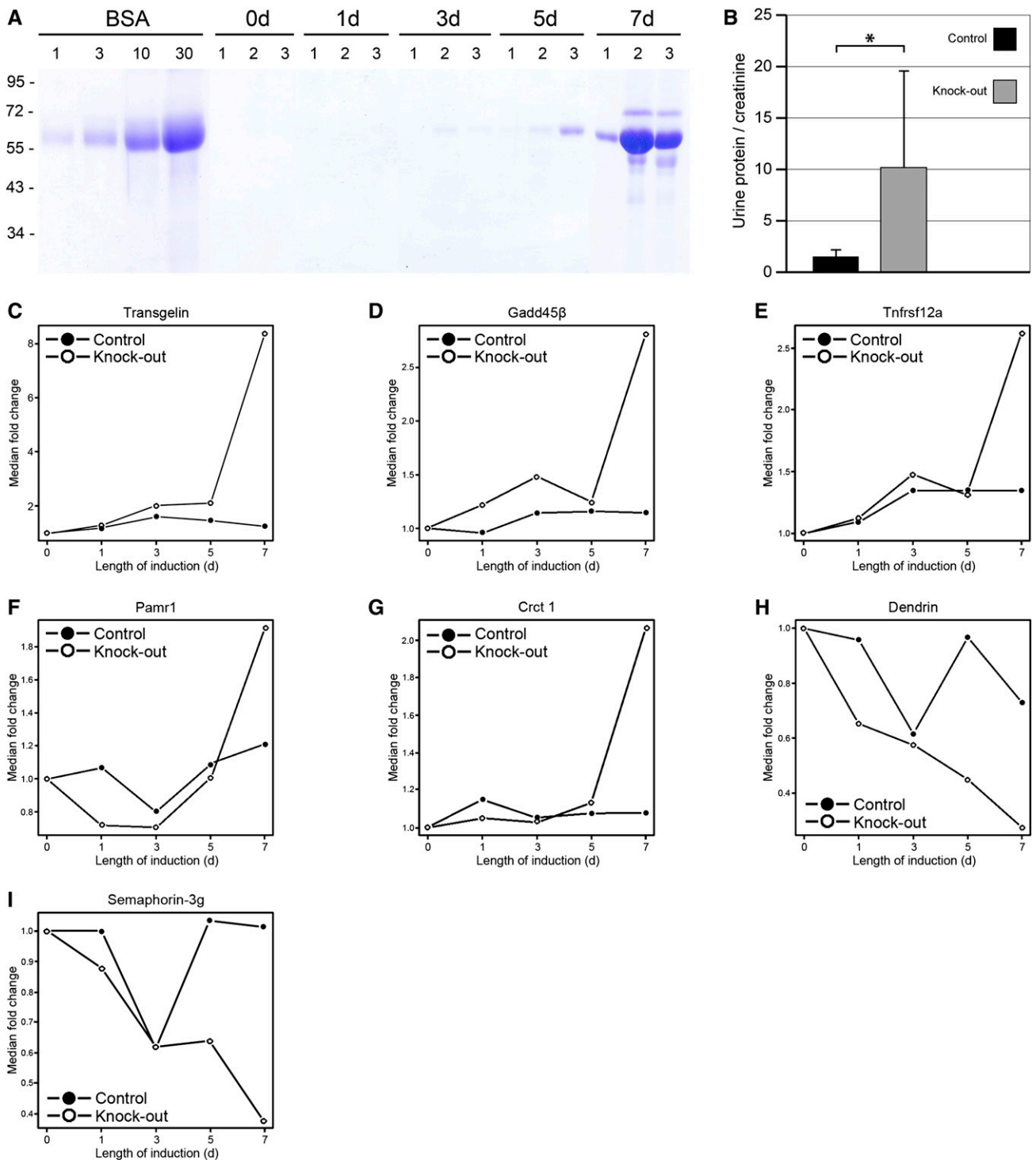


Figure 6. DNA microarray analysis of glomeruli after inactivation of *Lmx1b*. (A) Triple transgenic and *Lmx1b*^{lox/lox}; *NPHS2*:rtTA mice (three animals each) were administered 2 mg/ml doxycycline for 0, 1, 3, 5, and 7 days in the drinking water; 0.5 μ l urine was loaded on a protein gel, which was subsequently stained with Coomassie Brilliant Blue. It can be seen that mild albuminuria developed after 5 days and pronounced albuminuria developed after 7 days. Variable amounts (1, 3, 10, and 30 μ g) of BSA served as a comparison. (B) Urinary protein/creatinine ratio 7 days after the administration of doxycycline. (C–I) Glomeruli were isolated from the same animals shown in A, and total RNA was isolated and subjected to DNA microarray analysis. Shown are the median fold changes of the microarray data. * $P < 0.05$.

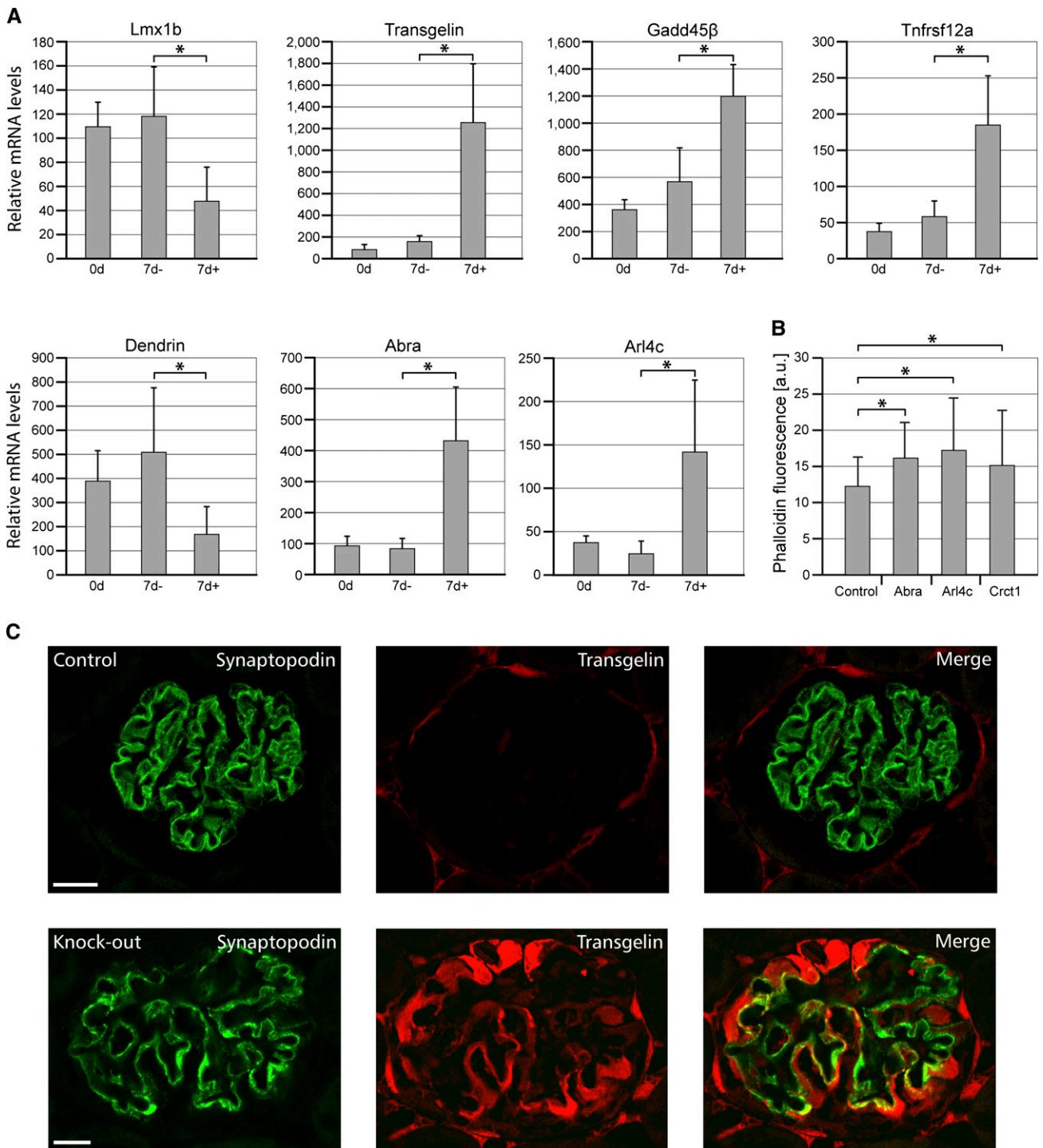


Figure 7. Expression analysis and functional characterization of *Lmx1b*-regulated genes. (A) Total RNA was isolated from freshly harvested glomeruli and subjected to quantitative real-time PCR. The following animals were used: five *Lmx1b*^{lox/lox}; *NPHS2*:rtTA; tetO: Cre mice receiving no doxycycline (0d), five *Lmx1b*^{lox/lox}; *NPHS2*:rtTA mice receiving 2 mg/ml doxycycline for 7 days (7d-), and five *Lmx1b*^{lox/lox}; *NPHS2*:rtTA; tetO:Cre mice receiving 2 mg/ml doxycycline for 7 days (7d+). (B) Transfection of primary podocytes with expression plasmids for *Abra*, *Arl4c*, and *Crct1* results in the increased formation of F-actin, which was shown by staining with fluorescently labeled phalloidin. (C) *Lmx1b*^{lox/lox}; *NPHS2*:rtTA (control) and triple transgenic mice (knockout) were treated with 2 mg/ml doxycycline for 7 days. Staining of kidney sections with antibodies against transgelin and synaptopodin reveals that the inactivation of *Lmx1b* leads to the synthesis of transgelin in podocytes. Shown are the mean values and SDs. Scale bar, 20 μ m. **P*<0.05.

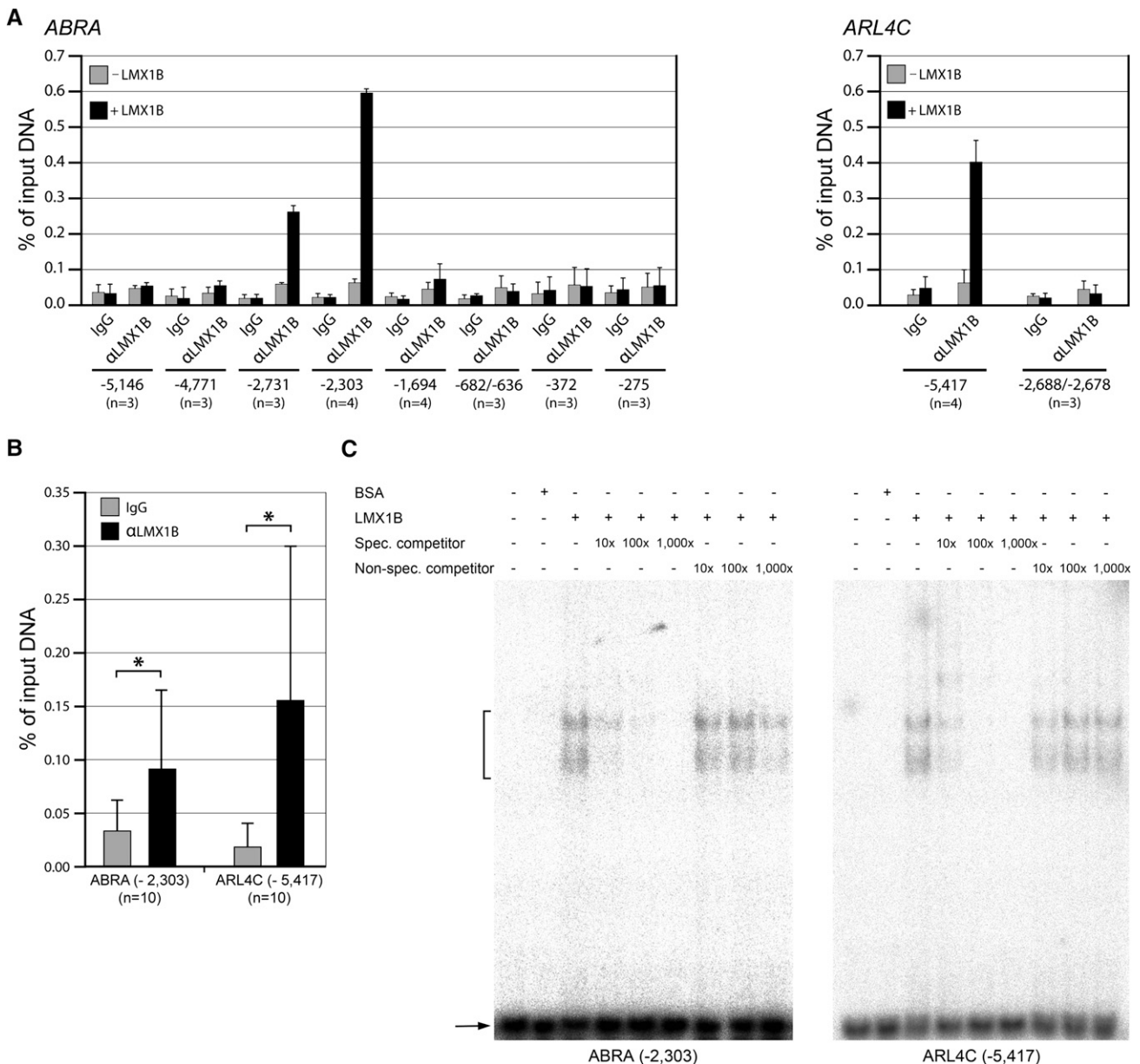


Figure 8. ChIP and gel shift experiments. (A) Stably transfected HeLa cells inducibly producing LMX1B were subjected to ChIP with the polyclonal rabbit anti-LMX1B antiserum BMO8 (α LMX1B). Regular rabbit IgG served as a negative control. Binding of LMX1B was shown for FLAT elements located at positions -2731 and -2303 of the *ABRA* gene and a FLAT element located at position -5417 of the *ARL4C* gene. (B) ChIP of conditionally immortalized human podocytes transiently transfected with an expression plasmid for human LMX1B was carried out under the same conditions as for the stably transfected HeLa cells. LMX1B recognizes the homologous FLAT elements as in HeLa cells. $*P < 0.05$. (C) Gel shift assays further support the binding of recombinant LMX1B protein to the indicated FLAT elements. BSA served as a negative control. The respective unlabeled oligonucleotides served as specific competitors, and a guanine and cytosine (GC)-rich region of the human *NPHS2* gene served as a nonspecific inhibitor. Shifted oligonucleotides are indicated by the bracket, and free probe is indicated by the arrow. Shown are the mean values and SDs, and the number of independent experiments is given in parentheses (A and B).

Knockdown of the *lmx1b* and *abra* Genes in Zebrafish Leads to Kidney Defects

To determine the relevance of our findings *in vivo*, we turned to the zebrafish as a model system. The zebrafish has been frequently used for the functional studies of genes involved in

renal development. Screening of the zebrafish genome (www.ensembl.org) led to the identification of one ortholog for *abra* and two orthologous genes for *arl4c* in zebrafish. All genes were expressed during zebrafish development and in adult tissues, although the individual expression patterns varied

(Supplemental Figure 3). This finding encouraged us to knock down the respective genes in zebrafish. Although strictly speaking, this process only allowed us to investigate the role of these genes during renal differentiation, we at least sought to obtain evidence for an interaction between them. The injection of antisense morpholinos against *arl4c* resulted in early embryonic death (Supplemental Figure 4), and therefore, these morpholinos were not included for additional analysis. However, the injection of antisense morpholinos against *lmx1b* and *abra* resulted in an increased body curvature, a coiled tail, and severe cardiac and body edema similar to what has been described when antisense morpholinos against *wt1* were injected.³⁸ The strength of the phenotypes varied in a dose-dependent manner, which allowed us to combine antisense morpholinos against *lmx1b* and *abra* to test for their genetic interaction. We found that a combination of antisense morpholinos resulted in a stronger gross morphologic phenotype than the injection of a single morpholino, again judged by body curvature and edema (Supplemental Figure 4). We, therefore, extended our experiments to the transgenic zebrafish line *wt1b::GFP*, which synthesizes GFP in the developing glomerulus and pronephric tubule.³⁸ Importantly, the combined knockdown of *lmx1b* and *abra* led to a more severe phenotype than the individual knockdown of *lmx1b* and *abra* alone. At 48 hours postfertilization, the frequency of zebrafish embryos with pronephros defects increased from ~10% (10.5% in *lmx1b* morphants and 12.8% in *abra* morphants) to 28.6% in combined *lmx1b/abra* morphants (Figure 9). The stronger effect observed after the combined knockdown of *lmx1b* and *abra* in developing zebrafish embryos supports the notion that LMX1B and ABRA act in a common

pathway *in vivo* and that *ABRA* is a target gene of LMX1B in podocytes.

DISCUSSION

Approximately 40% of the patients suffering from nail–patella syndrome develop nephrological symptoms, which result from defects in the podocytes and the glomerular basement membrane.² The identification of mutations in the *LMX1B* gene^{3–5} and the characterization of conventional *Lmx1b* knockout mice^{10–13} strongly argued that the transcription factor LMX1B is essential for the proper differentiation of podocyte precursors. Podocyte development in the conventional *Lmx1b* knockout mice arrests at the cuboidal stage without elaboration of foot processes and slit diaphragms; furthermore, the glomerular basement membrane is split. Because the $\alpha 3$ and $\alpha 4$ chains of collagen IV as well as the slit diaphragm protein podocin are absent in the glomeruli of conventional *Lmx1b* knockout mice, the *COL4A3*, *COL4A4*, and *NPHS2* genes have been considered promising target genes of LMX1B. However, these proteins are still present in the glomeruli of nail–patella syndrome patients,¹⁴ which argues against *COL4A3*, *COL4A4*, and *NPHS2* being direct targets of LMX1B.

The constitutive podocyte-specific inactivation of *Lmx1b* has unequivocally shown the essential role of LMX1B in podocytes.¹⁵ It seemed, however, that in those mice the foot processes and slit diaphragms disappeared after they had formed and that LMX1B, therefore, is necessary for podocytes to not only acquire their highly differentiated phenotype but also to

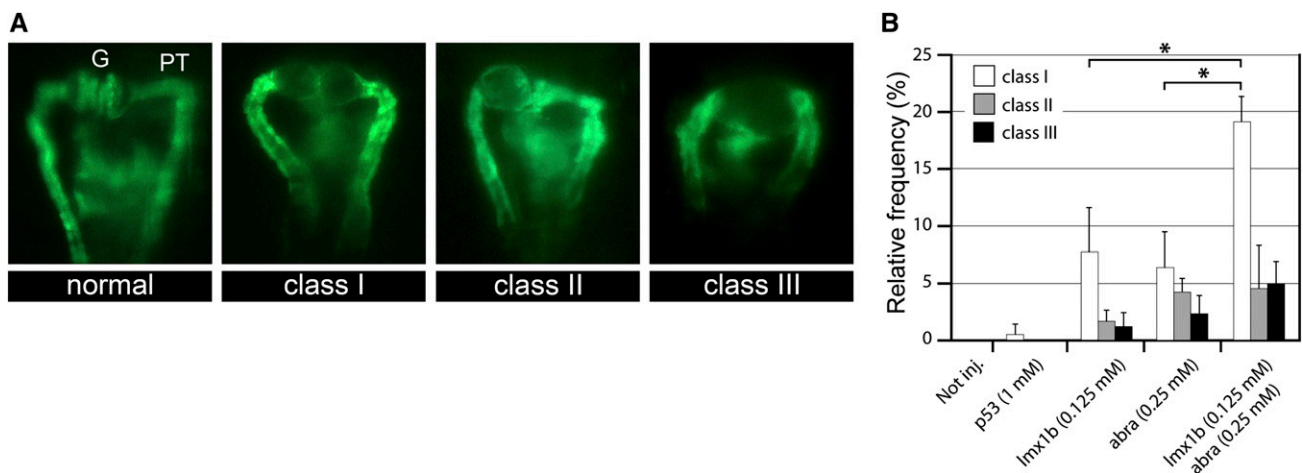


Figure 9. Knockdown of *lmx1b* and *abra* in zebrafish. (A) Representative images of normal and malformed pronephroi in transgenic *wt1b::GFP* zebrafish at 48 hours postfertilization. The normal pronephros consists of one (fused) glomerulus (G) and the pronephric tubule (PT). In *lmx1b* and *abra* morphants, three classes of phenotypes can be seen: symmetric cystic glomeruli (class I), asymmetric cystic glomeruli (class II), and pronephroi without a glomerulus (class III). Embryos are shown from a dorsal view, and the anterior end is at the top. (B) Quantitation of abnormal pronephroi after the injection of antisense morpholinos against *lmx1b* and *abra* based on the categories described in A. In the case of *lmx1b*, a combination of morpholinos against *lmx1b.1* and *lmx1b.2* was used, and each was at a concentration of 0.0625 mM. Shown are the mean values and SDs of four independent experiments. For each experiment, 40–50 embryos per morpholino were included. * $P < 0.05$.

maintain it. The results presented here and in previous publications^{12,13} clearly show that LMX1B serves both functions. Not only is *Lmx1b* present in the podocytes of adult mice,¹⁵ but the inducible inactivation of *Lmx1b* in adult mice also leads to the failure of the glomerular filtration barrier as evidenced by pronounced proteinuria. In both the constitutive¹⁵ and the inducible podocyte-specific *Lmx1b* knockout mice, various proteins of essential function for the glomerular filtration barrier such as podocin, nephrin, Cd2ap, α -actinin-4, Wt1, and the $\alpha 3$ and $\alpha 4$ chains of collagen IV, were still present at the time that albuminuria was observed. Similar to the situation in the kidneys of nail-patella syndrome patients,¹⁴ the leaky filtration barrier after the inactivation of *Lmx1b* cannot be explained by the absence of these proteins. Together with the facts that LMX1B failed to activate an *NPHS2* promoter fragment in reporter assays and that the endogenous *NPHS2* gene was not upregulated in stably transfected HeLa cells inducibly producing LMX1B,¹³ this finding at least casts doubt on the hypothesis that *NPHS2* is a target gene of LMX1B.

The data presented here offer an alternative explanation for the role of LMX1B in podocytes and possibly, other tissues as well. We routinely observe pronounced proteinuria 7 days after the administration of doxycycline. The elucidation of various hereditary diseases has taught us that proteinuria results from defects in the glomerular basement membrane, the slit diaphragm, and the actin cytoskeleton.³⁹ Because in the inducible *Lmx1b* knockout mice, collagen IV is still present 1 week after the inactivation of *Lmx1b* and the charge density of the glomerular basement membrane is the same with and without *Lmx1b*, we consider it unlikely that a defect in the glomerular basement membrane causes proteinuria. Furthermore, the downregulation of slit diaphragm proteins, such as nephrin and podocin, occurs after we observe pronounced proteinuria, and therefore, the loss of these proteins also cannot explain the observed phenotype. Our data rather argue that LMX1B regulates genes, which are associated with the actin cytoskeleton.

We very consistently noticed that more podocytes grew out of freshly isolated glomeruli after the inactivation of *Lmx1b*. The outgrowth of podocytes is a complex process, because the podocytes have to detach from the glomerular basement membrane and concomitantly establish new cell-matrix contacts on the culture dish. In a replating assay, we noticed a higher adhesiveness of primary podocytes to laminin after the inactivation of *Lmx1b*. Because a similar behavior was observed on additional substrates, such as poly-L-lysine, fibronectin, and collagen I (data not shown), it is not possible that a single integrin is responsible for this effect, because cell-matrix contacts to the various substrates are mediated by distinct integrins. The fact that the focal contact area and the spreading rate did not differ between podocytes without and with inactivated *Lmx1b* also argues against an involvement of integrins. Considering the decreased diffusion of integrins shown by nanoscale particle tracking, the increased phalloidin staining, and the delayed recovery after cytochalasin treatment

in the absence of *Lmx1b*, we consider it more likely that LMX1B regulates the actin cytoskeleton. On a molecular level, the upregulation of transgelin, *Abra*, and *Arl4c* after the inactivation of *Lmx1b* and the increased phalloidin staining in primary podocytes after the expression of *Abra*, *Arl4c*, and *Crct1* certainly support such a model. The synergistic effect of suboptimal doses of antisense morpholinos against *lmx1b* and *abra* during pronephros development in zebrafish argues along the same lines. In contrast to the *ABRA* and *ARL4C* genes, however, we found no binding sites for LMX1B in the promoter region of the *TAGLN* gene that we analyzed. Whether this finding indicates that the binding site for LMX1B is outside of the promoter region under investigation or that the *TAGLN* gene is nonspecifically activated because of podocyte damage will be subject to additional experiments.

Transgelin is an actin binding protein that stabilizes actin fibers.³⁰ *Abra* also is associated with the actin cytoskeleton and may stimulate F-actin formation and/or stabilize actin fibers.⁴⁰ *Arl4c* is poorly characterized so far, but it has been shown to recruit cytohesin-2 (*syn.* ARNO) to the plasma membrane,⁴¹ and cytohesin-2, in turn, interacts with the focal contact protein paxillin.⁴² We, therefore, argue that, in the absence of *Lmx1b*, podocytes contain a stiffer actin cytoskeleton, which may make the podocytes more vulnerable. A similar scenario has been proposed for the mechanism underlying hereditary forms of FSGS caused by mutations in *ACTN4*.²³ *ACTN4* encodes α -actinin-4, a protein associated with stress fibers. Missense mutations in α -actinin-4 result in a higher affinity of the mutant protein for stress fibers and a stiffer actin network.^{43,44} The importance of an intact actin cytoskeleton for podocytes is further supported by previous publications.^{24,27,45-49}

In addition to a dysregulated actin network, the downregulation of dendrin, a slit diaphragm-associated protein,^{32,33} may also contribute to the development of proteinuria, although the difference in expression levels between glomeruli with and without *Lmx1b* was not high. It has to be kept in mind, however, that *Lmx1b* mRNA levels only dropped to 40% after Cre-mediated recombination. In the original description of the P2.5-rtTA mice, Cre recombinase activity in most, but not all, podocytes was reported,¹⁶ which is consistent with our finding that *Lmx1b* mRNA levels had not dropped to zero. Obviously, there will be podocyte-to-podocyte variability in the mRNA levels of *Lmx1b* and in turn, its target genes. The strong proteinuria that we consistently observed after 7 days of doxycycline administration shows that intact podocytes cannot substitute for those podocytes with absent *Lmx1b* mRNA, which in turn, may also lose dendrin. Regrettably, we have not been able to detect *Lmx1b* in podocytes by immunostaining of kidney sections using various mono- and polyclonal anti-*Lmx1b* antibodies, and we, therefore, cannot perform double staining for *Lmx1b* and its target genes. The function of dendrin is poorly understood, but it is clear that an intact slit diaphragm is necessary to maintain the glomerular filtration barrier. It is noteworthy that, similar to the actin-associated protein synaptopodin,⁵⁰ dendrin is also present in

the brain⁵¹ and that *Lmx1b* is necessary for both the proper differentiation of podocytes and certain brain regions.⁵² The upregulation of the proapoptotic proteins *Gadd45β* and *Tnfrsf12a* certainly is consistent with the increased rate of apoptotic events after the inactivation of *Lmx1b*, but it remains to be determined whether these genes are directly regulated by *LMX1B* or are induced as part of the apoptotic process.

Considering the facts that nail–patella syndrome patients suffer from a variety of symptoms—dysmorphic finger and toe nails, dysplastic or absent patellae, renal abnormalities, and glaucoma²—and that the conventional *Lmx1b* knockout mice develop defects in multiple tissues,^{10,53–55} one has to wonder how *LMX1B* performs its task in tissues as diverse as the kidneys, the eyes, and the brain. It may well be that *LMX1B* interacts with different cofactors and accordingly, regulates distinct target genes in several cell types.³⁷ This interpretation is supported by the analysis of the gene expression pattern in the limb buds of *Lmx1b* knockout mice,^{56,57} because we see no overlap with our array data when we set a limit of at least a twofold up- or downregulation. One has to be cautious, however, to compare the data from different microarray experiments. Obviously, a more careful expression analysis is necessary to determine whether the target genes of *LMX1B* are distinct in various tissues. It is, therefore, also conceivable that *LMX1B* regulates more general cellular functions, such as actin-associated cell motility and cell matrix contacts, that are important in different cellular contexts. Such a scenario could readily explain the podocyte phenotypes observed in the different *Lmx1b* knockout mice, such as the cuboidal shape and the lack of foot processes and slit diaphragms in the conventional *Lmx1b* knockout mice.^{12,13} In this model, the absence of podocin and the $\alpha 3$ and $\alpha 4$ chains of collagen IV in the conventional *Lmx1b* knockout mice would be caused by the fact that the podocytes do not reach a certain (permissive) stage in development after which other genes are turned on; it is not because *NPHS2*, *COL4A3*, and *COL4A4* are direct target genes of *LMX1B*.

CONCISE METHODS

Mouse Strains, Genotyping, and Recombination Analysis

All mouse lines were maintained on a C57Bl/6 background. Mice with a floxed *Lmx1b* allele (provided by Randy Johnson) were generated by introducing loxP sites upstream and downstream of exons 4 and 6, respectively.¹⁵ LC-1 mice (provided by Hermann Bujard) contain a Cre recombinase and luciferase expression cassette under

control of the tet-operator,⁵⁸ and the P2.5-rtTA mice produce the rtTA protein under control of a *Nphs2* promoter fragment.¹⁶ Synthesis of Cre (and luciferase) was induced through the administration of 2 mg/ml doxycycline in the drinking water of triple transgenic mice.⁵⁹ The presence of the rtTA cassette was identified by Southern blot analysis. Presence of the Cre cassette and the floxed *Lmx1b* allele and recombination of the *Lmx1b* gene were determined by PCR using the primers given in Table 1.

Perfusion Fixation and Light and Electron Microscopy

Mice were fixed by perfusion through the distal abdominal aorta with 4% paraformaldehyde and 1× PBS for 3 minutes. Subsequently, kidney slices were fixed overnight in 4% paraformaldehyde and 1× PBS for paraffin embedding, and 2% glutaraldehyde and 1× PBS for electron microscopy. The latter specimens were incubated with cacodylate-buffered 1% OsO₄ for 2–3 hours before being embedded in Epon. Ultrathin sections were stained with uranyl acetate and lead citrate and then visualized in a transmission electron microscope (Zeiss EM 902) equipped with a cooled CCD digital camera (TRS Tröndle Restlichtverstärkersysteme).

The distribution of negatively charged molecules in the glomerular basement membrane was determined by incubating small pieces of freshly removed renal cortex for 30 minutes at room temperature in 0.5% polyethyleneimine and 0.9% NaCl (pH 7.3). The tissue was then washed three times for 10 minutes each in 50 mM sodium cacodylate (pH 7.3) before being fixed for 1 hour in 0.1% glutaraldehyde and 2% phosphotungstic acid. After again washing three times for 10 minutes each with 50 mM cacodylate buffer, the tissue was incubated for 2 hours at 4°C in 25 mM cacodylate buffer and 1% OsO₄ before being embedded in Epon. Ultrathin sections were stained with uranyl acetate and lead citrate and then visualized in the transmission electron microscope. Polyethyleneimine was obtained from Sigma (P3143), and phosphotungstic acid was from Fluka (79690).

Immunofluorescence Staining and Staining for Apoptotic Cells

Immunofluorescence staining of kidney sections for podocin, nephrin, Wt1, transgelin, synaptopodin, and the $\alpha 4$ chain of collagen IV was performed as described previously.¹⁵ Briefly, sections were deparaffinized, subjected to antigen retrieval treatment, and blocked overnight in 2% BSA and 1× PBS before the primary antibodies were applied. The following antibodies were used: the polyclonal rabbit anti-podocin antibody P35 (diluted 1:1,000),⁶⁰ a polyclonal rabbit anti-nephrin antibody (diluted 1:1,000),⁶¹ a polyclonal rabbit anti-WT1 antibody (diluted 1:500; sc-192; Santa Cruz Biotechnology), a polyclonal rabbit anti-transgelin antibody (diluted 1:1,000; ab 14106; Abcam), and the monoclonal mouse anti-synaptopodin antibody G1 (diluted 1:10).⁶² After three washes, the sections

Table 1. Oligonucleotides for PCR from genomic DNA

Target	Forward Primer (5'–3')	Reverse Primer (5'–3')
Cre	CCTGGAAATGCTTCTGTCCG	CAGGGTGTATAAGCAATCCC
Floxed <i>Lmx1b</i>	AGGCTCCATCCATTCTCTC	CCACAATAAGCAAGAGGCAC
Recombined <i>Lmx1b</i>	GTACCTCTGTGAGGATGCC	ACAGGGCAGAGGGAAAGTG

were stained with a Cy3-conjugated goat anti-rabbit IgG antibody (diluted 1:300; 111-165-045; Dianova) or a Alexa 488-conjugated goat anti-mouse IgG antibody (diluted 1:600; A11029; Invitrogen) for 1 hour at room temperature. For staining with a polyclonal rabbit anti-collagen IV $\alpha 4$ antibody (diluted 1:800),⁶³ 7- μm -thick cryosections of snap-frozen kidneys were fixed in ethanol for 10 minutes at -20°C and then air-dried. After incubation for 1 hour with 6 M urea and 0.1 M glycine (pH 3.5) at room temperature, the sections were blocked overnight with 5% nonfat dry milk solution. The next day, sections were washed with $1\times$ PBS and stained overnight with the anti-collagen IV $\alpha 4$ primary antibody.

TUNEL staining was performed on 7- μm -thick paraffin sections. After deparaffinization, the sections were first treated for 15 minutes with 20 $\mu\text{g}/\text{ml}$ proteinase K and then blocked for 30 minutes with 5% BSA, 20% FCS, and $1\times$ PBS before the TUNEL reaction mixture (Roche Applied Science) was added for 1 hour at 37°C . Stained sections were visualized on a confocal scanning microscope (Zeiss LSM 510 Meta). To visualize apoptotic events in primary podocytes, cells were fixed with 3% paraformaldehyde and $1\times$ PBS for 20 minutes at 4°C . After blocking and permeabilization with 3% BSA, 0.1% Triton X-100, and $1\times$ PBS, the podocytes were incubated overnight with a primary rabbit antibody directed against cleaved caspase-3 (diluted 1:100; 9661; Cell Signaling Technology). Specific staining was visualized with a secondary Alexa Fluor 468-conjugated donkey anti-rabbit antibody (diluted 1:600; A10042; Invitrogen).

Isolation of Primary Podocytes

Glomeruli were isolated from the kidneys of adult mice essentially as described in a previous publication.⁶⁴ Briefly, after mice were anaesthetized, the abdominal cavity and thorax were opened. Then, a syringe containing 40 ml magnetic bead suspension at a concentration of 2×10^6 beads/ml (140.11; Invitrogen Dynal) was inserted into the left ventricle, the abdominal aorta was cut open below the renal arteries, and the suspension was administered at a constant pressure of 60 mm Hg. The kidneys were taken out, decapsulated, and cut into small pieces, which were subsequently digested for 30 minutes at 37°C with 1 mg/ml collagenase A (103578; Roche Diagnostics). Subsequently, the digested kidney was pushed through a 100- μm cell strainer (352360; Becton-Dickenson) to remove larger pieces of tissue, and the filtrate was washed extensively using a magnet. Finally, the pure glomeruli were plated in DMEM/F-12 medium containing 10% FCS, 100 U penicillin/ml, 100 μg streptomycin/ml, and $1\times$ insulin/transferrin/selenium (F01510-0881; PAA) to allow outgrowth of podocytes.

Adhesion Assays with Primary Podocytes

Primary podocytes were detached with trypsin-EDTA or Accutase (L11-007; PAA) and resuspended in serum-free medium at a concentration of 450,000 cells/ml; 100 μl cell suspension was seeded in triplicate into the wells of a 96-well plate coated with different substrates. After incubating for 30 minutes at 37°C , the wells were washed with $1\times$ PBS, and a 50 μl substrate solution containing 3.75 mM 4-nitrophenyl N-acetyl- β -D-glucosaminide (N9376; Sigma), 50 mM sodium citrate (pH 5.0), and 0.25% Triton X-100 was added. The reaction was incubated overnight at 37°C and stopped

with 75 μl 50 mM glycine and 5 mM EDTA (pH 10.4), and the absorbance was measured at 405 nm. The experimental values were normalized to those values obtained when the washing step was omitted and the cells were allowed to attach overnight.

Electrophysiological Characterization of Podocytes

Patch-clamp experiments were performed on freshly isolated glomeruli and primary podocytes 12 days after plating. The patch membrane was perforated with nystatin (100 mg/ml; added to the pipette solution) to determine the membrane potential. Recordings were performed using a custom-made EPC-7-like amplifier (U. Fröbe, Institute of Physiology, Freiburg, Germany). The patch pipette solution contained 95 mM K-gluconate, 30 mM KCl, 4.8 mM Na_2HPO_4 , 1.2 mM NaH_2PO_4 , 5 mM glucose, 2.38 mM MgCl_2 , 0.726 mM CaCl_2 , 3 mM ATP, and 1 mM EGTA (pH 7.2). The solution for whole-cell experiments contained 145 mM NaCl, 1.6 mM K_2HPO_4 , 0.4 mM KH_2PO_4 , 1.3 mM Ca-gluconate, 1 mM MgCl_2 , 5 mM glucose, and 5 mM Hepes.

Electric Cell Substrate Impedance Sensing

Electric cell substrate impedance sensing (ECIS)⁶⁵ was used to quantify the kinetics of podocyte spreading on different extracellular matrix proteins. Cells were seeded on the surface of small gold-film electrodes deposited on the bottom of eight-well cell culture dishes. The ECIS instrumentation reads the electrode capacitance with non-invasive electric fields at an alternating current (AC) frequency of 32 kHz. When cells attach and spread on the electrode surface, the electrode capacitance drops from starting values of a cell-free electrode to those values of a cell-covered electrode, which correspond to a fully established cell layer. The drop in electrode capacitance is directly proportional to the fractional surface coverage of the electrode. Thus, the time course of the electrode capacitance mirrors the time course of cell spreading when a suspension of cells is seeded in the well.

To characterize the spreading of podocytes, electrodes (8w2e micro; Applied BioPhysics Inc., Troy, NY) were coated with either fibronectin or BSA (100 $\mu\text{g}/\text{ml}$) for 1 hour at room temperature. The commercial 8w2e micro electrodes were modified such that the working volume was reduced down to 30 μl . Glomeruli were isolated from triple transgenic and control mice, which had received 2 mg/ml doxycycline in the drinking water for 8 days. Five days after the glomeruli had been plated, primary podocytes were harvested in serum-free medium and plated in the wells of the electrode array (50,000 cells/well). Cell spreading was continuously monitored by reading the capacitance at 32 kHz using the ECIS 1600R device (Applied BioPhysics Inc.). To extract the rate of cell spreading, the individual datasets were differentiated in time. The spreading rates given in Figure 5A correspond to the maximum change in capacitance observed within the first 2 hours of the experiment.

Measurement of Focal Contact Area

Primary podocytes were harvested 5 days after the plating of glomeruli. The cells were plated onto coverslips coated for 1 hour with fibronectin at a concentration of 50 $\mu\text{g}/\text{ml}$. Podocytes were allowed to adhere overnight, and then the cells were fixed with 4% paraformaldehyde and $1\times$ PBS for 15 minutes at room temperature.

Focal contacts were visualized by staining with a primary mouse monoclonal anti-paxillin antibody (diluted 1:300; 610052; BD Transduction Laboratories) and a secondary FITC-coupled goat anti-mouse IgG antibody (diluted 1:200; 55493; ICN Biomedicals). Total cell area was determined by staining the actin cytoskeleton with rhodamine phalloidin (diluted 1:300; PHDR1; Cytoskeleton). Digital pictures of the green and red channels were quantitated using the ImageJ software package.⁶⁶ Focal contact area was expressed by relating the FITC-positive to the rhodamine-positive area.

Nanoscale Particle Tracking

Primary podocytes were harvested with Accutase 5 days after the isolation of glomeruli; 30,000 cells each were plated onto 35-mm Petri dishes and allowed to attach overnight. The next morning, cells were incubated with fibronectin-coated nanobeads for 30 minutes at 37°C before the movement of the beads was tracked for 5 minutes. Beads moved spontaneously with a mean square displacement (MSD) that followed a power law with time: $MSD = D \times (t/t_0)^\beta + c$. The evolution of the MSD over time, t , can be described by an apparent diffusivity, D , and the persistence of motion can be described by the power law exponent, β . The term c reflects the random noise from thermal and nonthermal sources, such as single myosin motors, and t_0 was arbitrarily set to 1 second. All parameters were determined by a least-squares fit.⁶⁷ Measurements of the spontaneous bead movements were performed after at least 30 minutes of incubation, which is sufficient to connect the beads to the cytoskeleton.⁶⁸ The specifics of the bead–cell connection matter little and do not influence the bead motion after the beads are firmly connected to the cytoskeleton.⁶⁹

Cytochalasin Treatment and Phalloidin Staining

Primary podocytes were exposed to 5 µg/ml cytochalasin D (A 7641; AppliChem) for 24 hours. Then, the cells were washed two times with fresh medium and allowed to recover at 37°C and 5% CO₂ in a Zeiss LSM 710 laser scanning microscope. Pictures were taken every 60 seconds, and cell size was determined with the Image J software

package. To visualize the F-actin cytoskeleton, cells were fixed overnight at 4°C with 4% paraformaldehyde and 1× PBS. Then, the podocytes were washed two times with 1× PBS and stained for 1 hour with Acti-stain 555 (diluted 1:400; PHDH1; Cytoskeleton).

DNA Microarray Analysis

Fourteen-week-old female triple transgenic and *Lmx1b^{lox/lox}; NPHS2:rtTA* mice were administered 2 mg/ml doxycycline for 0, 1, 3, 5, and 7 days (three animals each per group). Glomeruli were isolated with magnetic beads, and total RNA was isolated with the PrepEase RNA SVE Spin Kit (USB). Samples were processed for microarray analysis by the regional German Affymetrix Service Provider and Microarray Core Facility, KFB—Center of Excellence for Fluorescent Bioanalytics (Regensburg, Germany). Hybridizations were carried out on Affymetrix Mouse Gene 1.0 ST Arrays in an Affymetrix Fluidics Station FS450, and the fluorescent signals were measured with an Affymetrix GeneChip Scanner 3000–7G. Gene expression profiles were background-corrected and normalized to probe level using the variance stabilization method described previously⁷⁰ as implemented in the Bioconductor suite of life science-related extensions release 2.4⁷¹ for the statistical computing environment R version 2.9.2.⁷² Normalized probe intensities were summarized into gene expression levels using an additive model⁷³ fitted by the median polish method.⁷⁴ Differential gene expression analysis was performed using linear models for microarrays generated with the Bioconductor package limma.⁷⁵

Quantitative RT-PCR

Quantitative PCR was performed as previously described¹⁵ using 10 ng cDNA and the oligonucleotides listed in Table 2. Data were normalized to S9 ribosomal (mouse) and Lamin A/C mRNA (human) and expressed as relative mRNA levels.

Generation of Stably Transfected HeLa Cells

An oligonucleotide encoding the Myc epitope NH₂-EQKLISEEDL-COOH was inserted at the 5' end of the human LMX1B cDNA in the

Table 2. Oligonucleotides for quantitative RT-PCR

mRNA	Forward Primer (5'–3')	Reverse Primer (5'–3')
Abra (z)	TGGGGGCAAAAAGGACATCGAG	ATCCTCACTGAAGGGGTTTCAGC
Arl4c (m)	TTTAAGAACCATAGGCAGAAATCA	CAATCTTCTAAGGATCGGGTTTC
Arl4c.1 (z)	ACCGGCTTGAGGAAGCCAAAAC	AGACCTCAAGGATTTGGGGAG
Arl4c.2 (z)	GCTGAAAACCAAGGAACGCCAC	TCACCTATGATGGCACAGGCTG
Crct1 (m)	CCTACAGAGCTTCTCCGGAAC	GCCGGTCTTCTGTTACTA
Dendrin (m)	AATGGAGAGGCCTTGAACCT	TCTCTGCCAAAAGTTCTCT
Ef1a (z)	AAGAGAACCATCGAGAAGTTCGA	ACCCAGGCGTACTTGAAGGA
Gadd45β (m)	CTGCCTCCTGGTCACGAA	TTGCCTCTGCTCTTTCACA
Lamin A/C (h)	TGCGTACGGCTCTCATCAACT	CTCGTCGTCCTCAACCACAGT
Lmx1b (h, m)	GAGCAAAGATGAAGAAGCTGGC	GGCCACGATCTGCTGCTG
Lmx1b.1 (z)	AATGCGCCGTGTGTCAACAACC	AGCGCCCGCATCACAAATTCTG
Lmx1b.2 (z)	AGAGAGAAAGATCTCGCCAGCC	GCTGTCATCACTGCCTTTTCCC
S9 (m)	GCAAGATGAAGCTGGATTAC	GGGATGTTACCACCTG
Stars (m)	AGGAGAGGCCTGAGCAAGA	GAGTGTCTCAGAGTACCTGTTTG
Tnfrsf12a (m)	ATTCGGCTTGGTGTGTGATG	CCATGCACCTGTGCGAGGTC
Transgelin (h)	GGCCAAGGCTCTACTGTCTG	CCCTTGTTGGCCATGTCT
Transgelin (m)	GCAGTGTGCCCTGATGTA	TCACCAATTTGCTCAGAATCAC

z, zebrafish mRNA; m, murine mRNA; h, human mRNA.

Table 3. Oligonucleotides for quantitative ChIP-PCR

Target	Forward Primer (5'–3')	Reverse Primer (5'–3')
hAbra (–5164)	GACACAATGGGGAAAGGGTA	GAAATCCAACCTTCCAGCA
hAbra (–4771)	AACAAAACAAAAGGGCAACC	TTTAAATGAAGTATTTGTCTTTCTGC
hAbra (–2731)	ATCTGCTGACATCCCCAAC	GATTTTCCTGCTGCTGCTGTC
hAbra (–2303)	TCAGATGCCGTTGAACTCTG	GCCGCTATTCGTTTTTCATC
hAbra (–1694)	GCTGAGCCCTGGACATTTT	TGGAAAGACAAGCATGTGGA
hAbra (–682/–636)	AAAATTTTGACTCCCTTTTGTATT	GCCCAGATACGAGAAAGACC
hAbra (–372)	GGAATAAAAGGAGGCACACG	AGCAGCCCTCAGTACAGCTC
hAbra (–275)	CTGGGGTTTAAAGTGGGAACA	CCAAGTGCCAGAGTGGAAAT
hArl4c (–5417)	TCCCTGCTGCACTGTAGAAA	TGCAGGTGAACTGAAATGCT
hArl4c (–2688/–2678)	CACCTGGTGAGTGAATTAGCA	ACCATGATGGGGTTTAGCAA

context of the expression plasmid pUHD 10–3. HeLa cells expressing the tetracycline-dependent transactivator⁷⁶ were transfected with 8 μ g expression plasmids pUHD 10–3/mycLMX1B together with 0.8 μ g selection plasmid. Positive clones were identified by Western blot analysis with the monoclonal anti-Myc epitope antibody 9E10.³⁷

Transient Transfection of Primary Podocytes and Conditionally Immortalized Human Podocytes

Primary podocytes were plated at a density of 20,000 cells on 10-mm coverslips. The next morning, cells were transfected with 1 μ g plasmid and 2 μ l Lipofectamine 2000 (Invitrogen) in a total volume of 100 μ l. Four hours later, the transfection mixture was removed, and new medium was added.

A conditionally immortalized human podocyte cell line⁷⁷ was grown in RPMI 1640, 10% FCS, and 1% insulin-transferrin-selenite (ITS) (41400–045; Gibco). One day after plating, the cells were transfected with an expression plasmid encoding the Myc epitope-tagged LMX1B protein. Forty-eight hours after transfection, the cells were subjected to ChIP.

ChIP

ChIP assays were performed as described previously.³⁷ Briefly, cells were fixed for 10 minutes at room temperature with 1% formaldehyde and DMEM. After rinsing with 1 \times PBS, the remaining formaldehyde was blocked by incubating for 5 minutes at room temperature with 125 mM glycine and 1 \times PBS. The cells were washed again with 1 \times PBS, scraped off the Petri dish, and centrifuged for 5 minutes at 860 \times g and 4°C. The cell pellet was resuspended in 100 mM NaCl, 50 mM Tris (pH 8.0), 5 mM EDTA, 0.5% SDS, 0.001% aprotinin, 0.001% leupeptin, and 1 mM PMSF and then sonicated 10 times for 30 seconds each with 30-second pauses in between (30% output level; sonicator Bandelin Sonoplus GM 2070). Immunoprecipitation was carried out with the rabbit polyclonal anti-LMX1B antiserum BMO8¹⁵ and rabbit IgG as a negative control. After reversing the crosslinking, the immunoprecipitated genomic DNA fragments were characterized by quantitative real-time PCR using the primers listed in Table 3.

Gel Shift Assay

Gel shift assays were performed essentially according to standard protocols.⁷⁸ Histidine-tagged full-length human LMX1B protein was produced in the *Escherichia coli* strain Rosetta (DE3) pLysS; 250 ng recombinant LMX1B protein was incubated with ³²P-labeled double-stranded oligonucleotides and then run on a 5% polyacrylamide gel.

The following oligonucleotides were used: human *ABRA* (–2303), 5'-AGA TTA AGT ATT AAA TCA CTT C-3' and 5'-GAA GTG ATT TAA TAC TTA ATC T-3'; human *ARL4C* (–5417), 5'-AGT AAG CTT AAT TAA ATG AAA A-3' and 5'-TTT TCA TTT AAT TAA GCT TAC T-3'; and human *NPHS2* (–287), 5'-CCT GCC CGG GGC CGG CTC TCC CAC-3' and 5'-GTG GGA GAG CCG GCC CCG GGC AGG-3'. Nonlabeled double-stranded oligonucleotides served as competitors.

Zebrafish Experiments

Zebrafish embryos were collected from the wild-type TüAB strain or a transgenic line containing the *wt1b::GFP* cassette.³⁸ Staging of the embryos was done according to standard procedures.⁷⁹ Antisense morpholino-oligonucleotides (GeneTools) were directed against an exon-splice donor site (*abra*) or the translational start site (*arl4c*). Morpholinos against *lmx1b* were described previously.⁸⁰ A morpholino targeting the Δ 113 isoform of p53, which is not expressed before 48 hours post-fertilization, served as a negative control⁸¹ (sequences are shown in Table 4). All morpholinos were dissolved in Danieus' buffer at a stock concentration of 2 mM. Dose–response experiments were carried out by injecting one- to four-cell embryos with \sim 5 nl diluted morpholinos; 24, 48, and 72 hours postfertilization, injected embryos were treated with 0.016% tricaine (Sigma) before being evaluated for morphologic defects using the epifluorescence microscope Zeiss Stereo Discovery V8. On determination of the lowest morpholino concentration required to induce morphologic defects, combined injections were performed. Images were generated using the AxioVision software (Zeiss).

ACKNOWLEDGMENTS

We are grateful for the gifts of materials from Corinne Antignac (anti-podocin antibody), Hermann Bujard (LC-1 mice), Larry Holzman

Table 4. Sequences of antisense morpholinos

Target	Morpholino (5'–3')
<i>abra</i> e1i1spl MO	cagaactcacCCAGGAACAGAGGAC
<i>arl4c.1</i> ATG MO	TATGATGAATATATAACGATCGATA
<i>arl4c.2</i> ATG MO	TGATGTCCTCGTTTGAGGGGTTAT
<i>lmx1b.1</i> ATG MO	CTTCGATTTTTATACCGTCCAACAT
<i>lmx1b.2</i> ATG MO	CCTCAATTTTGATTCCGTCAGCAT
<i>p53</i> ATG MO	GCGCCATTGCTTTGCAAGAATTG

(anti-nephrin antibody), Randy Johnson (floxed *Lmx1b* mice), Jeff Miner (anti-collagen IV $\alpha 4$ antibody), Peter Mundel (antisynaptopodin antibody), and Moin Saleem (conditionally immortalized human podocytes). Carina Mirbeth provided superb technical assistance. We thank Christina Ebert for the maintenance of the zebrafish colony. Achim Göpferich kindly permitted access to the confocal laser scanning microscope. Ton Maurer skillfully arranged the figures.

Financial support from German Research Council Grant SFB 699 is gratefully acknowledged.

DISCLOSURES

None.

REFERENCES

- Raschle A, Suleiman H, Neumann T, Witzgall R: Role of transcription factors in podocytes. *Nephron Exp Nephrol* 106: e60–e66, 2007
- Sweeney E, Fryer A, Mountford R, Green A, McIntosh I: Nail patella syndrome: A review of the phenotype aided by developmental biology. *J Med Genet* 40: 153–162, 2003
- Dreyer SD, Zhou G, Baldini A, Winterpacht A, Zabel B, Cole W, Johnson RL, Lee B: Mutations in *LMX1B* cause abnormal skeletal patterning and renal dysplasia in nail patella syndrome. *Nat Genet* 19: 47–50, 1998
- McIntosh I, Dreyer SD, Clough MV, Dunston JA, Eyaid W, Roig CM, Montgomery T, Ala-Mello S, Kaitila I, Winterpacht A, Zabel B, Frydman M, Cole WG, Francomano CA, Lee B: Mutation analysis of *LMX1B* gene in nail-patella syndrome patients. *Am J Hum Genet* 63: 1651–1658, 1998
- Vollrath D, Jaramillo-Babb VL, Clough MV, McIntosh I, Scott KM, Lichter PR, Richards JE: Loss-of-function mutations in the LIM-homeodomain gene, *LMX1B*, in nail-patella syndrome. *Hum Mol Genet* 7: 1091–1098, 1998
- Dunston JA, Hamlington JD, Zaveri J, Sweeney E, Sibbring J, Tran C, Malbroux M, O'Neill JP, Mountford R, McIntosh I: The human *LMX1B* gene: Transcription unit, promoter, and pathogenic mutations. *Genomics* 84: 565–576, 2004
- Bongers EMHF, Gubler M-C, Knoers NVAM: Nail-patella syndrome. Overview on clinical and molecular findings. *Pediatr Nephrol* 17: 703–712, 2002
- Del Pozo E, Lapp H: Ultrastructure of the kidney in the nephropathy of the nail-patella syndrome. *Am J Clin Pathol* 54: 845–851, 1970
- Ben-Bassat M, Cohen L, Rosenfeld J: The glomerular basement membrane in the nail-patella syndrome. *Arch Pathol* 92: 350–355, 1971
- Chen H, Lun Y, Ovchinnikov D, Kokubo H, Oberg KC, Pepicelli CV, Gan L, Lee B, Johnson RL: Limb and kidney defects in *Lmx1b* mutant mice suggest an involvement of *LMX1B* in human nail patella syndrome. *Nat Genet* 19: 51–55, 1998
- Morello R, Zhou G, Dreyer SD, Harvey SJ, Ninomiya Y, Thorner PS, Miner JH, Cole W, Winterpacht A, Zabel B, Oberg KC, Lee B: Regulation of glomerular basement membrane collagen expression by *LMX1B* contributes to renal disease in nail patella syndrome. *Nat Genet* 27: 205–208, 2001
- Miner JH, Morello R, Andrews KL, Li C, Antignac C, Shaw AS, Lee B: Transcriptional induction of slit diaphragm genes by *Lmx1b* is required in podocyte differentiation. *J Clin Invest* 109: 1065–1072, 2002
- Rohr C, Prestel J, Heidet L, Hosser H, Kriz W, Johnson RL, Antignac C, Witzgall R: The LIM-homeodomain transcription factor *Lmx1b* plays a crucial role in podocytes. *J Clin Invest* 109: 1073–1082, 2002
- Heidet L, Bongers EMHF, Sich M, Zhang S-Y, Loirat C, Meyrier A, Broyer M, Landthaler G, Faller B, Sado Y, Knoers NVAM, Gubler M-C: *In vivo* expression of putative *LMX1B* targets in nail-patella syndrome kidneys. *Am J Pathol* 163: 145–155, 2003
- Suleiman H, Heudobler D, Raschle A-S, Zhao Y, Zhao Q, Hertting I, Vitzthum H, Moeller MJ, Holzman LB, Rachel R, Johnson R, Westphal H, Raschle A, Witzgall R: The podocyte-specific inactivation of *Lmx1b*, *Ldb1* and *E2a* yields new insight into a transcriptional network in podocytes. *Dev Biol* 304: 701–712, 2007
- Shigehara T, Zaragoza C, Kitiyakara C, Takahashi H, Lu H, Moeller M, Holzman LB, Kopp JB: Inducible podocyte-specific gene expression in transgenic mice. *J Am Soc Nephrol* 14: 1998–2003, 2003
- Remuzzi G, Bertani T: Pathophysiology of progressive nephropathies. *N Engl J Med* 339: 1448–1456, 1998
- Harvey SJ, Miner JH: Revisiting the glomerular charge barrier in the molecular era. *Curr Opin Nephrol Hypertens* 17: 393–398, 2008
- Harvey SJ, Jarad G, Cunningham J, Rops AL, van der Vlag J, Berden JH, Moeller MJ, Holzman LB, Burgess RW, Miner JH: Disruption of glomerular basement membrane charge through podocyte-specific mutation of agrin does not alter glomerular permselectivity. *Am J Pathol* 171: 139–152, 2007
- Kreidberg JA, Donovan MJ, Goldstein SL, Rennke H, Shepherd K, Jones RC, Jaenisch R: $\alpha 3 \beta 1$ integrin has a crucial role in kidney and lung organogenesis. *Development* 122: 3537–3547, 1996
- Kanasaki K, Kanda Y, Palmsten K, Tanjore H, Lee SB, Lebleu VS, Gattone VH Jr, Kalluri R: Integrin $\beta 1$ -mediated matrix assembly and signaling are critical for the normal development and function of the kidney glomerulus. *Dev Biol* 313: 584–593, 2008
- Pozzi A, Jarad G, Moeckel GW, Coffa S, Zhang X, Gewin L, Eremina V, Hudson BG, Borza D-B, Harris RC, Holzman LB, Phillips CL, Fassler R, Quaggin SE, Miner JH, Zent R: $\beta 1$ integrin expression by podocytes is required to maintain glomerular structural integrity. *Dev Biol* 316: 288–301, 2008
- Kaplan JM, Kim SH, North KN, Rennke H, Correia LA, Tong H-Q, Mathis BJ, Rodríguez-Pérez J-C, Allen PG, Beggs AH, Pollak MR: Mutations in *ACTN4*, encoding α -actinin-4, cause familial focal segmental glomerulosclerosis. *Nat Genet* 24: 251–256, 2000
- Brown EJ, Schlöndorff JS, Becker DJ, Tsukaguchi H, Tonna SJ, Uscinski AL, Higgs HN, Henderson JM, Pollak MR: Mutations in the formin gene *INF2* cause focal segmental glomerulosclerosis. *Nat Genet* 42: 72–76, 2010
- Boyer O, Benoit G, Gribouval O, Nevo F, Tête M-J, Dantal J, Gilbert-Dussardier B, Touchard G, Karras A, Presne C, Grunfeld J-P, Legendre C, Joly D, Rieu P, Mohsin N, Hannedouche T, Moal V, Gubler M-C, Brouin I, Mollet G, Antignac C: Mutations in *INF2* are a major cause of autosomal dominant focal segmental glomerulosclerosis. *J Am Soc Nephrol* 22: 239–245, 2011
- Huber TB, Kwok C, Wu H, Asanuma K, Gödel M, Hartleben B, Blumer KJ, Miner JH, Mundel P, Shaw AS: Bigenic mouse models of focal segmental glomerulosclerosis involving pairwise interaction of CD2AP, Fyn, and synaptopodin. *J Clin Invest* 116: 1337–1345, 2006
- Garg P, Verma R, Cook L, Soofi A, Venkatarreddy M, George B, Mizuno K, Gurniak C, Witke W, Holzman LB: Actin-depolymerizing factor cofilin-1 is necessary in maintaining mature podocyte architecture. *J Biol Chem* 285: 22676–22688, 2010
- Schwab A, Hanley P, Fabian A, Stock C: Potassium channels keep mobile cells on the go. *Physiology (Bethesda)* 23: 212–220, 2008
- Frisch T, Thoumine O: Predicting the kinetics of cell spreading. *J Biomech* 35: 1137–1141, 2002
- Assinder SJ, Stanton J-A, Prasad PD: Transgelin: An actin-binding protein and tumour suppressor. *Int J Biochem Cell Biol* 41: 482–486, 2009
- Chorianopoulos E, Heger T, Lutz M, Frank D, Bea F, Katus HA, Frey N: FGF-inducible 14-kDa protein (Fn14) is regulated via the RhoA/ROCK kinase pathway in cardiomyocytes and mediates nuclear factor- κ B activation by TWEAK. *Basic Res Cardiol* 105: 301–313, 2010
- Patrakka J, Xiao Z, Nukui M, Takemoto M, He L, Oddsson A, Perisic L, Kaukinen A, Szigartyo CA, Uhlén M, Jalanko H, Betsholtz C, Tryggvason

- K: Expression and subcellular distribution of novel glomerulus-associated proteins dendrin, ehd3, sh2d4a, plekhh2, and 2310066E14Rik. *J Am Soc Nephrol* 18: 689–697, 2007
33. Asanuma K, Campbell KN, Kim K, Faul C, Mundel P: Nuclear relocation of the nephrin and CD2AP-binding protein dendrin promotes apoptosis of podocytes. *Proc Natl Acad Sci U S A* 104: 10134–10139, 2007
 34. Nakayama M, Ishidoh K, Kojima Y, Harada N, Kominami E, Okumura K, Yagita H: Fibroblast growth factor-inducible 14 mediates multiple pathways of TWEAK-induced cell death. *J Immunol* 170: 341–348, 2003
 35. Yoo J, Ghiassi M, Jirmanova L, Balliet AG, Hoffman B, Fornace AJ Jr, Liebermann DA, Böttinger EP, Roberts AB: Transforming growth factor- β -induced apoptosis is mediated by Smad-dependent expression of GADD45b through p38 activation. *J Biol Chem* 278: 43001–43007, 2003
 36. German MS, Wang J, Chadwick RB, Rutter WJ: Synergistic activation of the insulin gene by a LIM-homeo domain protein and a basic helix-loop-helix protein: Building a functional insulin minienhancer complex. *Genes Dev* 6: 2165–2176, 1992
 37. Rasche A, Neumann T, Raschta A-S, Neumann A, Heining E, Kastner J, Witzgall R: The LIM-homeodomain transcription factor LMX1B regulates expression of NF- κ B target genes. *Exp Cell Res* 315: 76–96, 2009
 38. Perner B, Englert C, Bollig F: The Wilms tumor genes *wt1a* and *wt1b* control different steps during formation of the zebrafish pronephros. *Dev Biol* 309: 87–96, 2007
 39. Pavenstädt H, Kriz W, Kretzler M: Cell biology of the glomerular podocyte. *Physiol Rev* 83: 253–307, 2003
 40. Arai A, Spencer JA, Olson EN: STARS, a striated muscle activator of Rho signaling and serum response factor-dependent transcription. *J Biol Chem* 277: 24453–24459, 2002
 41. Hofmann I, Thompson A, Sanderson CM, Munro S: The Arl4 family of small G proteins can recruit the cytohesin Arf6 exchange factors to the plasma membrane. *Curr Biol* 17: 711–716, 2007
 42. Torii T, Miyamoto Y, Sanbe A, Nishimura K, Yamauchi J, Tanoue A: Cytohesin-2/ARNO, through its interaction with focal adhesion adaptor protein paxillin, regulates preadipocyte migration via the downstream activation of Arf6. *J Biol Chem* 285: 24270–24281, 2010
 43. Weins A, Kenlan P, Herbert S, Le TC, Villegas I, Kaplan BS, Appel GB, Pollak MR: Mutational and biological analysis of α -actinin-4 in focal segmental glomerulosclerosis. *J Am Soc Nephrol* 16: 3694–3701, 2005
 44. Ward SM, Weins A, Pollak MR, Weitz DA: Dynamic viscoelasticity of actin cross-linked with wild-type and disease-causing mutant α -actinin-4. *Biophys J* 95: 4915–4923, 2008
 45. Asanuma K, Kim K, Oh J, Giardino L, Chabanis S, Faul C, Reiser J, Mundel P: Synaptopodin regulates the actin-bundling activity of α -actinin in an isoform-specific manner. *J Clin Invest* 115: 1188–1198, 2005
 46. Jones N, Blasutig IM, Eremina V, Ruston JM, Bladt F, Li H, Huang H, Larose L, Li SS-C, Takano T, Quaggin SE, Pawson T: Nck adaptor proteins link nephrin to the actin cytoskeleton of kidney podocytes. *Nature* 440: 818–823, 2006
 47. Garg P, Verma R, Nihalani D, Johnstone DB, Holzman LB: Nephrin cooperates with nephrin to transduce a signal that induces actin polymerization. *Mol Cell Biol* 27: 8698–8712, 2007
 48. Zhu J, Sun N, Aoudjit L, Li H, Kawachi H, Lemay S, Takano T: Nephrin mediates actin reorganization via phosphoinositide 3-kinase in podocytes. *Kidney Int* 73: 556–566, 2008
 49. Faul C, Donnelly M, Merscher-Gomez S, Chang YH, Franz S, Delfgaauw J, Chang J-M, Choi HY, Campbell KN, Kim K, Reiser J, Mundel P: The actin cytoskeleton of kidney podocytes is a direct target of the anti-proteinuric effect of cyclosporine A. *Nat Med* 14: 931–938, 2008
 50. Mundel P, Heid HW, Mundel TM, Krüger M, Reiser J, Kriz W: Synaptopodin: An actin-associated protein in telencephalic dendrites and renal podocytes. *J Cell Biol* 139: 193–204, 1997
 51. Neuner-Jehle M, Denizot J-P, Borbély AA, Mallet J: Characterization and sleep deprivation-induced expression modulation of dendrin, a novel dendritic protein in rat brain neurons. *J Neurosci Res* 46: 138–151, 1996
 52. Dai J-X, Johnson RL, Ding Y-Q: Manifold functions of the nail-patella syndrome gene *Lmx1b* in vertebrate development. *Dev Growth Differ* 51: 241–250, 2009
 53. Chen H, Ovchinnikov D, Pressman CL, Aulehla A, Lun Y, Johnson RL: Multiple calvarial defects in *Lmx1b* mutant mice. *Dev Genet* 22: 314–320, 1998
 54. Pressman CL, Chen H, Johnson RL: *LMX1B*, a LIM homeodomain class transcription factor, is necessary for normal development of multiple tissues in the anterior segment of the murine eye. *Genesis* 26: 15–25, 2000
 55. Smidt MP, Asbreuk CHJ, Cox JJ, Chen H, Johnson RL, Burbach JPH: A second independent pathway for development of mesencephalic dopaminergic neurons requires *Lmx1b*. *Nat Neurosci* 3: 337–341, 2000
 56. Krawchuk D, Kania A: Identification of genes controlled by LMX1B in the developing mouse limb bud. *Dev Dyn* 237: 1183–1192, 2008
 57. Gu WXW, Kania A: Identification of genes controlled by LMX1B in E13.5 mouse limbs. *Dev Dyn* 239: 2246–2255, 2010
 58. Schöning K, Schwenk F, Rajewsky K, Bujard H: Stringent doxycycline dependent control of CRE recombinase *in vivo*. *Nucleic Acids Res* 30: e134, 2002
 59. Gallagher AR, Schöning K, Brown N, Bujard H, Witzgall R: Use of the tetracycline system for inducible protein synthesis in the kidney. *J Am Soc Nephrol* 14: 2042–2051, 2003
 60. Roselli S, Gribouval O, Boute N, Sich M, Benessy F, Attié T, Gubler M-C, Antignac C: Podocin localizes in the kidney to the slit diaphragm area. *Am J Pathol* 160: 131–139, 2002
 61. Holzman LB, St John PL, Kovari IA, Verma R, Holthofer H, Abrahamson DR: Nephrin localizes to the slit pore of the glomerular epithelial cell. *Kidney Int* 56: 1481–1491, 1999
 62. Mundel P, Gilbert P, Kriz W: Podocytes in glomerulus of rat kidney express a characteristic 44 KD protein. *J Histochem Cytochem* 39: 1047–1056, 1991
 63. Miner JH, Sanes JR: Collagen IV α 3, α 4, and α 5 chains in rodent basal laminae: Sequence, distribution, association with laminins, and developmental switches. *J Cell Biol* 127: 879–891, 1994
 64. Takemoto M, Asker N, Gerhardt H, Lundkvist A, Johansson BR, Saito Y, Betsholtz C: A new method for large scale isolation of kidney glomeruli from mice. *Am J Pathol* 161: 799–805, 2002
 65. Wegener J, Keese CR, Giaever I: Electric cell-substrate impedance sensing (ECIS) as a noninvasive means to monitor the kinetics of cell spreading to artificial surfaces. *Exp Cell Res* 259: 158–166, 2000
 66. Schneider CA, Rasband WS, Eliceiri KW: NIH Image to Image J: 25 years of image analysis. *Nat Methods* 9: 671–675, 2012
 67. Raupach C, Zitterbart DP, Mierke CT, Metzner C, Müller FA, Fabry B: Stress fluctuations and motion of cytoskeletal-bound markers. *Phys Rev E Stat Nonlin Soft Matter Phys* 76: 011918, 2007
 68. Mierke CT, Frey B, Fellner M, Herrmann M, Fabry B: Integrin α 5 β 1 facilitates cancer cell invasion through enhanced contractile forces. *J Cell Sci* 124: 369–383, 2011
 69. Metzner C, Raupach C, Zitterbart DP, Fabry B: Simple model of cytoskeletal fluctuations. *Phys Rev E Stat Nonlin Soft Matter Phys* 76: 021925, 2007
 70. Huber W, von Heydebreck A, Sültmann H, Poustka A, Vingron M: Variance stabilization applied to microarray data calibration and to the quantification of differential expression. *Bioinformatics* 18 [Suppl 1]: S96–S104, 2002
 71. Gentleman RC, Carey VJ, Bates DM, Bolstad B, Dettling M, Dudoit S, Ellis B, Gautier L, Ge Y, Gentry J, Hornik K, Hothorn T, Huber W, Iacus S, Irizarry R, Leisch F, Li C, Maechler M, Rossini AJ, Sawitzki G, Smith C, Smyth G, Tierney L, Yang JYH, Zhang J: Bioconductor: Open software development for computational biology and bioinformatics. *Genome Biol* 5: R80, 2004

72. R Development Core Team: *R: A Language and Environment for Statistical Computing*, Vienna, Austria, R Foundation for Statistical Computing, 2008
73. Irizarry RA, Bolstad BM, Collin F, Cope LM, Hobbs B, Speed TP: Summaries of Affymetrix GeneChip probe level data. *Nucleic Acids Res* 31: e15, 2003
74. Tukey JW: *Exploratory Data Analysis*, Reading, MA, Addison-Wesley, 1977
75. Smyth GK: Limma: Linear models for microarray data. In: *Bioinformatics and Computational Biology Solutions Using R and Bioconductor*, edited by Gentleman R, Carey V, Dudoit S, Irizarry R, Huber W, New York, Springer, 2005
76. Gossen M, Bujard H: Tight control of gene expression in mammalian cells by tetracycline-responsive promoters. *Proc Natl Acad Sci U S A* 89: 5547–5551, 1992
77. Saleem MA, O'Hare MJ, Reiser J, Coward RJ, Inward CD, Farren T, Xing CY, Ni L, Mathieson PW, Mundel P: A conditionally immortalized human podocyte cell line demonstrating nephrin and podocin expression. *J Am Soc Nephrol* 13: 630–638, 2002
78. Ausubel FA, Brent R, Kingston RE, Moore DD, Seidman JG, Smith JA, Struhl K: *Current Protocols in Molecular Biology*, New York, John Wiley & Sons, 1996
79. Kimmel CB, Ballard WW, Kimmel SR, Ullmann B, Schilling TF: Stages of embryonic development of the zebrafish. *Dev Dyn* 203: 253–310, 1995
80. O'Hara FP, Beck E, Barr LK, Wong LL, Kessler DS, Riddle RD: Zebrafish *Lmx1b.1* and *Lmx1b.2* are required for maintenance of the isthmic organizer. *Development* 132: 3163–3173, 2005
81. Robu ME, Larson JD, Nasevicius A, Beiraghi S, Brenner C, Farber SA, Ekker SC: p53 activation by knockdown technologies. *PLoS Genet* 3: e78, 2007

This article contains supplemental material online at <http://jasn.asnjournals.org/lookup/suppl/doi:10.1681/ASN.2012080788/-/DCSupplemental>.